4 siRNAライブラリーの利用

松本佐保姫　宮岸 真　多比良和誠

はじめに

RNAi（RNA interference：RNA干渉）とは，二本鎖のRNA（double-stranded RNA：dsRNA）を細胞内に導入することで，その相補配列のmRNAが切断され，その結果遺伝子の発現が抑制されるという現象であり，簡便に高効率に遺伝子の発現を抑制する手法として注目されてきている．近年のヒトゲノム計画の進展により，人類の遺伝情報が次々と明らかにされる中で，その多くの遺伝情報は，機能が未解明のままである．これらの遺伝子の網羅的な機能解析への試みは今までもなされており，われわれの研究室を含め，ランダムリボザイムライブラリーを用いた手法などが開発され，多くの成果を挙げてきている．こうした流れの中で，RNAiの技術を用いたライブラリースクリーニングが注目されている．

われわれのグループを含むいくつかのグループで，RNAiを用いたライブラリーの作製が行われ，遺伝子の網羅的解析に対する試みが進められている[1)～5)]．本項では，siRNA発現ベクターライブラリーを用いた遺伝子の解析についてその具体的方法を紹介したい．

原理とストラテジー

RNAiを用いたライブラリーを作製する場合には，化学的に合成したsiRNAを用いる場合と，ベクターを細胞に導入してsiRNAを発現させる場合の2つが考えられる．化学的に合成したsiRNAを用いる場合には，抑制効果が一過的にしか持続しない，細胞によっては導入が困難である，コストがかかるなどの問題がある．われわれのグループでは，siRNA発現ベクターを用いることで，安定した遺伝子の発現抑制効果をもつライブラリーの作製に成功した（3章-3参照）．siRNA発現ベクターシステムは，センス鎖とアンチセンス鎖がループを描くヘアピン（ステムループ）タイプと，直鎖状のタンデムタイプに分けることができる．ヘアピンタイプでは，ヘアピン型の転写産物が細胞内のRNase（Dicer）によってプロセッシングされsiRNAとなる．タンデムタイプでは2つのプロモーターから各々センス鎖とアンチセンス鎖に相当するRNAを転写し，細胞内でハイブリダイズして，二本鎖のsiRNAとなる．これら2つのタイプのベクターを比較すると，低濃度ではヘアピンタイプの方がより高い遺伝子抑制効果をもつことが示された[6)]．しかし，ヘアピンタイプは，反復配列が存在する

ために，大腸菌内で不安定であり変異などが入りやすい．われわれは，センス鎖に点変異を入れることで，活性を維持したまま安定したベクターを作製することに成功した．さらに，ループ配列についてもより活性の高いものを見出した．現在，この最適化された安定なベクターシステム（piGENE™hU6ベクター，iGENE社）を用いて，ライブラリーを用いたスクリーニング系の研究が進行中である[6) 7)]

以下に，siRNA発現ベクターライブラリーを用いた，dsRNAによるアポトーシス経路の網羅的解析法について述べる．

準備するもの

1）siRNA発現ベクターライブラリー

・ターゲットサイトの選択

翻訳領域を主にターゲットサイトとして選び，独自のアルゴリズムに基づいて1つの遺伝子に対して2ヵ所以上のターゲットサイトを選択している

・siRNA発現ベクター

ヘアピンタイプで，ヒトU6プロモーターを発現プロモーターとするpc PUR hU6[8)]を用いた．このベクター系は，TaKaRa社，TOYOBO社で受託販売を行っている

2）細胞

・HeLa S3

・スクリーニングに適した細胞の選択

表現型が見やすいもの，取り扱いやすいものが望ましい

3）試薬

・培地（DMEM＋10% FBS）

・Lipofectamine 2000（Invitrogen社）

・puromycin（和光純薬）

・FuGENE™6 Transfection Reagent（Roche社）

・poly（I：C）（Amersham Biosciences社）

・PBS（－）

・0.2%クリスタルバイオレット

4）ネガティブコントロールとなるsiRNA発現ベクター

プロトコール

1．siRNA発現ベクターライブラリーの細胞へのトランスフェクション

HeLa S3細胞にLipofectamine 2000を用いてベクターをトランスフェクションする（試薬に添付のプロトコールを参照）．1ウェル当たり細胞と同量の1ベクターをトランスフェクションする❶

2．ピューロマイシンでのセレクション❷

トランスフェクションして36時間後，1 mg/mlのピューロマ

❶この際，ネガティブコントロールのsiRNA発現ベクターも同様にトランスフェクションする．

❷今回使用したベクターは，ピューロマイシン耐性であり，ピューロマイシンを加えることで，トランスフェクションされている細胞のみが生き残りセレクションすることができる．

イシンでトランスフェクションされた細胞のみセレクションする．この際，ピューロマイシン耐性ではないベクターをトランスフェクションしたものにも同様にピューロマイシンを加える❸

❸ ピューロマイシンセレクションの陰性コントロールとなる．

3．播き換え

24時間後，陰性コントロールの細胞が完全に全滅したことを顕微鏡で確認

▼

1ウェルを同細胞数ずつ48ウェルプレートの3ウェルに播き換える

4．アポトーシスの誘導

播き換え12時間後に，poly（I：C）❹を0.5 μg/ウェルずつFuGENE6でトランスフェクションする（試薬に添付のプロトコールを参照）

❹ dsRNAとしてpoly（I：C）を用い，インターフェロン応答によりアポトーシスを誘導する．

5．クリスタルバイオレットで染色

アポトーシス誘導24時間後に細胞をPBS（－）で洗う

▼

細胞を固定し0.2%クリスタルバイオレットで染色する

《注意》違う細胞を用いる場合にはピューロマイシンでのセレクションの条件や，アポトーシス導入条件などの再検討が必要である．

トラブルシューティング

トラブル	考えられる原因	解決のための処置
ピューロマイシンのセレクションが不十分	細胞密度が濃すぎる	細胞密度の条件を振ってみて陰性コントロールが十分に全滅する条件を検討する
	ピューロマイシンの濃度が低すぎる	ピューロマイシンの濃度を検討する
ピューロマイシンを加えると生き残る細胞数が少なすぎる	細胞密度が薄すぎる	細胞密度の条件の再検討をする
	ピューロマイシンの濃度が高すぎる	ピューロマイシンの濃度を検討する
	ベクターのトランスフェクション効率が低い	トランスフェクション試薬を変えてみる．トランスフェクション条件を再検討する
アポトーシスの誘導後，染色しても陰性と陽性の差がはっきりしない	細胞密度が濃すぎるもしくは薄すぎる	細胞数を振ってみる
	アポトーシス誘導条件が強すぎる	poly（I：C）の量を再検討する

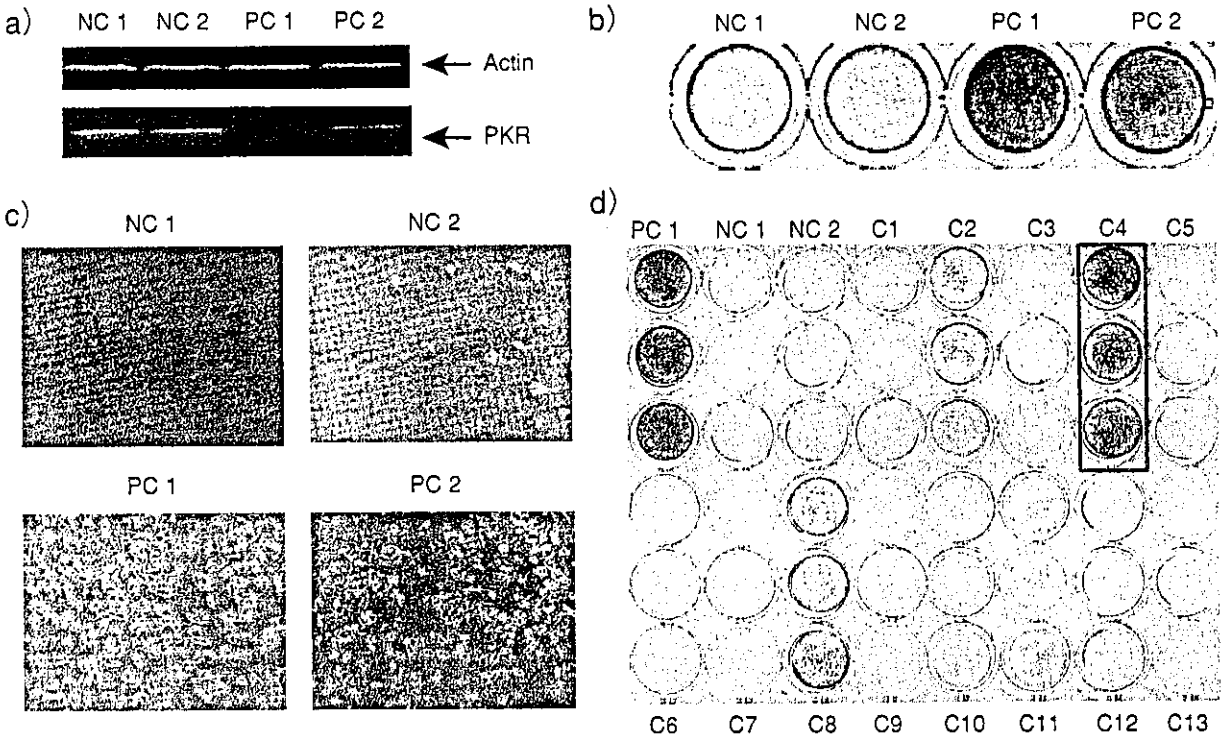

図1 PKRノックダウンによるアポトーシスの抑制およびスクリーニング実験例

a) PKRの異なる2つのサイトに対するsiRNA発現ベクターをトランスフェクションしたサンプルをPC 1, PC 2（陽性コントロール 1, 2），Renilla luciferaseの異なる2つのサイトに対するsiRNA発現ベクターをトランスフェクションしたサンプルをNC 1, NC 2（陰性コントロール 1, 2）として，タンパク質を回収し，ウエスタンブロッティングした

b) NC，PCそれぞれにdsRNAでアポトーシスを誘導し，24時間後に細胞を洗浄のうえ，クリスタルバイオレットで染色したもの．生き残った細胞のみが紫色に染色されている

c) b）のプレートを顕微鏡撮影したもの

d) プロトコールの方法にてスクリーニングを行い，クリスタルバイオレットで染色したプレート．C1からC13は，PKR，Renilla luciferaseとは異なる遺伝子に対するsiRNA発現ベクターをトランスフェクションした後，アポトーシスを誘導したもの．太線で囲ったC4は，細胞が生き残っておりdsRNAによるアポトーシスを阻害している（巻頭カラー口絵⓫参照）

実験例

PKR（プロテインキナーゼR）がdsRNAによるアポトーシスに関与していることはすでに知られている．そこで，PKRをスクリーニングの陽性コントロールとした．まず，PKRに対するsiRNA発現ベクターを2種類（PC1，PC2）作製し，細胞にトランスフェクションした．これらのsiRNA発現ベクターが十分にタンパク質の発現を抑制しているかどうかをウエスタンブロッティングで確認した．図1aに示すように，PC1ではほぼ完全にPKRはノックダウンされておりPC2も十分に抑制されていることがわかる．PKRに対するsiRNA発現ベクターをトランスフェクションした後，プロトコールに示す方法で，dsRNAによるアポトーシスを誘導し，クリスタルバイオレットで染色した（図1b，c）．陰性コントロールでは，ほとんどの細胞がアポトーシスを起こしているのに対し，PKRをノックダウンした細胞は生き残っていることがわかる．これらの結果から，PKRをノックダウンすることで，dsRNAによるアポトーシスが抑制されたことが示された．このPKRを陽性コントロール，Renilla luciferaseに対するsiRNA発現ベクターを陰性コントロールとして，プロトコールに

示す方法にてスクリーニングを行った例を図1dに示す．図1dではC1～C13までの13種類の異なる遺伝子に対するsiRNA発現ベクターを作製し，細胞にトランスフェクションのうえ，アポトーシスを誘導している．図に示すように，C4では，アポトーシスが抑制されており，C4がdsRNAによるアポトーシスに関連する因子であることが示唆される．

おわりに

以上述べてきたように，RNAiは目的の遺伝子を特異的・効率的に簡便に抑制する方法として，その有用性が注目されてきた．今後は，RNAiによるノックダウン技術を用いて，遺伝子の網羅的解析を行う動きがますます加速することが予想される．そこで問題となるのは，RNAiのより効率的なデリバリーシステムと，遺伝子抑制の特異性である．ウイルスベクターが導入効率の高さから注目されるが，特に，レトロウイルスベクター，レンチウイルスベクターはゲノム中に組み込まれるため，恒常的なsiRNAの発現が期待できる．安全性が確立すれば，これらウイルス系のsiRNA発現ベクターが広く有用なものとなるであろう．RNAiの特異性に関しては，研究が進むにつれて必ずしも一般的な現象であるといえないことがわかってきた．ターゲット遺伝子と数塩基のミスマッチを有していても遺伝子抑制効果を示す場合もあり，また，導入したsiRNAの量が多い場合にはoff-target効果[9]（3章-2参照）やインターフェロン応答（1章-2参照）といった非特異的な抑制効果を示す場合もありうる．このようなRNAiの非特異的な効果を回避するためには，優れたアルゴリズムを使って適切なサイトを選択することが重要なポイントとなってくる．また，同一の遺伝子の異なる部位をターゲットとして複数のsiRNAを作製するなど，適切なコントロールを置くことも非常に重要である．さらに，ノックダウンした遺伝子に対するレスキュー実験を行う必要もあるだろう．

今後，より安定した遺伝子抑制効果や，高い特異性が実現することで，RNAi研究がさらに大きな成果を生物学研究の領域にもたらすことが期待される．本項で紹介したライブラリーはアポトーシス関連の数百の遺伝子に対してのみであったが，今後，キナーゼ・ホスファターゼ・転写因子に対するライブラリーを順次作製し，AIST/NEDO siRNA expression LibraryとしてAIST/NEDO（産業技術総合研究所／新エネルギー・産業技術総合開発機構）から一般の日本の研究者に配布する予定である．本項で紹介したsiRNAベクターライブラリーを用いた機能的スクリーニングによって，今後数多くの研究者が，生理的現象を明らかにすることを期待している．

参考文献

1）Sen, G. et al. : Nat. Genet., 36 : 183-189, 2004
2）Shirane, D. et al. : Nat. Genet., 36 : 190-196, 2004
3）Zheng, L. et al. : Proc. Natl. Acad. Sci. USA, 101 : 135-140, 2004
4）Aza-Blanc, P. et al. : Mol. Cell, 12 : 627-637, 2003
5）Berns, K. et al. : Nature, 25 : 431-437, 2004
6）Miyagishi, M. & Taira, K. : Oligonucleotides, 13 : 325-333, 2003
7）Miyagishi, M. et al. : Virus Res., 102 : 117-124, 2004
8）Miyagishi, M. & Taira, K. : Nat. Biotechnol., 20 : 497-500, 2002
9）Jackson, A. L. et al. : Nat. Biotechnol., 21 : 635-637, 2003

THE JOURNAL OF BIOLOGICAL CHEMISTRY

Vol. 280, No. 1, Issue of January 7, pp. 826–831, 2005
Printed in U.S.A.

Identification of a Network Involved in Thapsigargin-induced Apoptosis Using a Library of Small Interfering RNA Expression Vectors*[S]

Received for publication, August 30, 2004
Published, JBC Papers in Press, October 14, 2004, DOI 10.1074/jbc.M409948200

Takashi Futami‡, Makoto Miyagishi§¶‖, and Kazunari Taira‡§**

From the ‡Department of Chemistry and Biotechnology, School of Engineering, The University of Tokyo, Hongo, Tokyo 113-8656, Japan and the §Gene Function Research Center, National Institute of Advanced Industrial Science and Technology, Central 4, 1-1-1 Higashi, Tsukuba Science City 305-8562, Japan

We describe here the construction of a library of small interfering RNA expression vectors targeted to a few hundred apoptosis-related genes and the application of this library to an investigation of thapsigargin (TG)-induced apoptosis. Thapsigargin triggers endoplasmic reticulum stress, with subsequent apoptosis, but the molecular mechanisms underlying this process are incompletely understood. Using our library, we identified three anti-apoptotic genes, namely, *NOXA*, *E2F1*, and *MAPK1*, in addition to already characterized genes in the apoptotic pathway. In contrast to proposals by others, our data revealed (i) that TG-induced apoptosis is associated with Apaf1 in a caspase-3- and caspase-9-independent manner; (ii) that the *E2F1-PUMA* pathway might be involved; and (iii) that the ERK pathway, via MAP3K8 (mitogen-activated protein kinase kinase 8), is required for the induction by TG of apoptosis. Our study demonstrates clearly that unexpected and novel genes can be identified effectively by our method, and it provides evidence for the efficacy and utility of the comprehensive analysis of signaling networks and pathways using a library of small interfering RNA expression vectors.

Although the human genome has been sequenced, the functions of many genes remain unknown. Phenotypic analysis using gene silencing appears to be an effective strategy in efforts to understand gene functions, and exploitation of RNA interference (RNAi)[1] appears to be a novel and powerful approach to the silencing of specific genes (1). RNAi is an intrinsic and evolutionarily conserved phenomenon in plants and animals whereby double-stranded RNA induces the sequence-specific degradation of homologous RNA (2).

Genome-wide RNAi screening in *Caenorhabditis elegans* and *Drosophila* cells, using libraries of double-stranded RNAs, has been demonstrated to be extremely useful in efforts to identify genes that regulate various processes and has enhanced our understanding of various biological processes (3–6). However, two major problems are associated with such screening in mammalian cells. First, double-stranded RNA induces an antiviral response that can result in cell death (7). However, Tuschl and co-workers (8) demonstrated that 21- and 22-nucleotide small interfering RNAs (siRNAs) can induce RNAi in the absence of an antiviral response in cultured mammalian cells. Subsequently, various groups, including our own, have developed systems for vector-mediated specific RNAi in mammalian cells (9–16). The second problem is that the effectiveness of siRNA is strongly dependent on the target sites in target RNAs. To generate a high quality library, we developed an original algorithm that allows us to predict favorable target sites (17). Using this algorithm and our optimized siRNA expression system (17), we are now constructing an siRNA expression library that will encompass the complete array of transcripts from the human genome. In this study, for construction of our first siRNA library, we focused on an apoptotic pathway and generated a library targeted to apoptosis-related genes. We used this library to screen for genes involved in endoplasmic reticulum (ER) stress-dependent apoptosis induced by thapsigargin (TG), a plant-derived sesquiterpene lactone.

EXPERIMENTAL PROCEDURES

Culture and Transfection of Cells—HCT116 cells were cultured in McCoy's 5A medium, supplemented with 10% fetal bovine serum and 1% penicillin/streptomycin. Transfections of siRNA expression vectors were performed using Lipofectamine™ 2000 (Invitrogen) according to the manufacturer's protocol.

Construction of a Library for Expression of U6-driven siRNA—We prepared siRNA vectors using the vector piGENE PURhU6 (17), which contains a human U6 promoter, a puromycin resistance gene, and two BspMI sites, which are used as sites for cloning a short hairpin sequence. For construction of siRNA vectors, we synthesized oligonucleotides with hairpin, terminator, and overhanging sequences. We annealed these fragments and inserted them into the BspMI sites of piGENE PURhU6. We based the sequences that we inserted immediately downstream of each U6 promoter on the results of application of our algorithm (17). Each vector was designed to express a short hairpin RNA in transfected cells.

Western Blotting Analysis—Preparation of cell lysates, Western blot-

* This work was supported by various grants from the National Institute of Advanced Industrial Science and Technology and from the New Energy and Industrial Technology Development Organization. The costs of publication of this article were defrayed in part by the payment of page charges. This article must therefore be hereby marked "*advertisement*" in accordance with 18 U.S.C. Section 1734 solely to indicate this fact.

[S] The on-line version of this article (available at http://www.jbc.org) contains a Supplemental Table.

¶ Present address: 21st Century Programs, Graduate School of Medicine, The University of Tokyo, Hongo, Tokyo 113-8655, Japan.

‖ To whom correspondence may be addressed: Dept. of Chemistry and Biotechnology, School of Engineering, The University of Tokyo, Hongo, Tokyo 113-8656, Japan. Tel./Fax: 81-3-5841-8828; E-mail: makoto-m@chembio.t.u-tokyo.ac.jp.

** To whom correspondence may be addressed: Dept. of Chemistry and Biotechnology, School of Engineering, The University of Tokyo, Hongo, Tokyo 113-8656, Japan. Tel./Fax: 81-3-5841-8828; E-mail: taira@chembio.t.u-tokyo.ac.jp.

[1] The abbreviations used are: RNAi, RNA interference; siRNA, small interfering RNA; ER, endoplasmic reticulum; TG, thapsigargin; ERK, extracellular signal-regulated kinase; z, benzyloxycarbonyl; fmk, fluoromethyl ketone; MAPK, mitogen-activated protein kinase; MAP3K8, mitogen-activated protein kinase kinase kinase 8; JNK, c-Jun amino-terminal kinase.

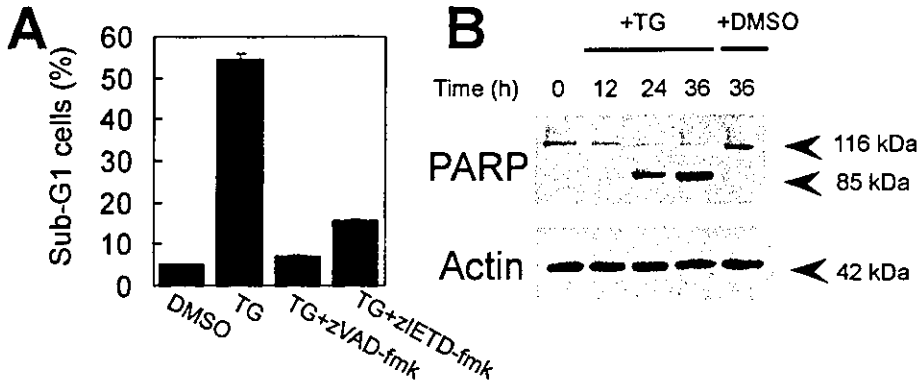

FIG. 1. **Thapsigargin induces caspase-dependent apoptosis in HCT116 cells.** *A*, flow cytometric analysis of DNA fragmentation induced by TG. HCT116 cells were incubated for 36 h with 1 μM TG or vehicle (dimethyl sulfoxide, *DMSO*) with or without 50 μM z-VAD-fmk or z-IETD-fmk. After treatment, the cells were harvested, permeabilized, stained with propidium iodide, and analyzed by fluorescence-activated cell sorter. The percentage of events within the sub-G_1 peak, which represents the population of apoptotic cells, was calculated using CellQuest software (BD Biosciences). The data are the means + S.E. of results from three separate experiments. *B*, Western blotting analysis of the cleavage of poly(ADP-ribose) polymerase (*PARP*) during treatment of cells with TG or vehicle (dimethyl sulfoxide, *DMSO*). Whole cell extracts of cells treated for the indicated times with 1 μM TG or vehicle (dimethyl sulfoxide) were analyzed. The Membranes were probed with the antibodies specific for the indicated proteins.

ting, and immunodetection were performed as described previously (18). Antibodies against caspase-3, caspase-8, capsase-9, Bid, poly(ADP-ribose) polymerase, ERK1/2, and phospho-ERK1/2 (Cell Signaling Technology), DR5 (CHEMICON), PUMA (ProSci Inc.), E2F1 (Santa Cruz), caspase-7 (BD PharMingen), and actin (Sigma) were used as suggested by the respective manufacturers. Second antibodies conjugated to horseradish peroxidase were obtained from Amersham Biosciences.

Flow Cytometry Analysis—Harvested cells aliquots (10^6 cells/assay) were permeabilized with 0.2% Triton-X100, centrifuged, and resuspended in phosphate-buffered saline that contained RNase A for 5 min at room temperature, and then propidium iodide (final concentration, 50 μg/ml) was added to the suspension. Fluorescence was monitored with flow cytometer (Becton Dickinson).

Materials—TG, z-VAD-fmk, and z-VAD-IETD were purchased from Calbiochem.

RESULTS

Construction of the siRNA Expression Vector Library—Prior to the construction of the siRNA expression library, we optimized our siRNA expression system. We constructed three types of siRNA vector system, namely, tandem-type, dual promoter-type, and hairpin-type, and compared the activities of the siRNAs. We determined that the hairpin-type system had the highest suppressive activity for low copy number plasmids. However, we observed a high rate of mutation in the stem-loop region when plasmids were used to transform *Escherichia coli*. This phenomenon was a serious problem with respect to the construction of a reliable library of siRNA vectors. We found that introduction of multiple C to T (or A to G) mutations into the sense strand rendered the plasmids genetically stable and did not affect silencing activity (17). Moreover, we optimized the loop sequence that connected sense and antisense sequences and other parameters that might affect the activity of the siRNA. Furthermore, we developed an algorithm for selection of effective target sequences (17). Together, the optimization of the siRNA expression system and the development of the algorithm enabled us to construct a large scale and high quality library of siRNA vectors.

Thapsigargin-induced Caspase-dependant Apoptosis—We focused on the ER stress-induced apoptotic pathway as the target of our initial siRNA expression library. We chose 241 apoptosis-related genes, including genes for kinases, caspases, transcription factors, and other already characterized genes that are known to be associated with various apoptotic pathways. To take off-target effects into account (19), we constructed siRNA vectors directed at two target sites within each gene. Although there are many reports of the involvement of a number of specific genes in ER stress-induced apoptosis, the signal transduction pathway remains to be fully defined. Therefore, to clarify the details of the ER stress-induced apoptotic pathway, we screened the siRNA expression library for siRNA that targeted genes that might be involved in TG-induced apoptosis. First, we confirmed that cell death caused by TG is, in fact, apoptosis under our experimental conditions. TG clearly induced apoptotic cell death in human colon carcinoma HCT116 cells, as demonstrated by fluorescence-activated cell sorter analysis, during which we observed a characteristic sub-G_1 peak, indicative of DNA fragmentation and a hallmark of apoptosis, in the case of TG-treated cells (Fig. 1*A*). Moreover, cleavage of anti-poly(ADP-ribose) polymerase, another hallmark of apoptosis, occurred 24 h after the start of treatment of cells with TG (Fig. 1*B*).

Incubation of cells with both TG and a pan-caspase inhibitor, z-VAD-fmk or the caspase-8 inhibitor z-IETD-fmk significantly blocked the appearance of the sub-G_1 peak, indicating that the apoptotic process was caspase-dependent and, specifically, caspase-8-dependent. We also examined the possible role of a death receptor (DR5), which is involved in the induction of apoptosis via the recruitment and the cleavage of caspase-8, in TG-induced apoptosis in HCT116 cells. Recent studies have implicated the death receptor (DR5) pathway in TG-induced apoptosis in several lines of cancer cells (20). TG induced the expression of the DR5 protein, which became apparent 12 h after the onset of treatment, and "knockdown" experiments using an siRNA vector targeted to DR5 mRNA revealed that the DR5 apoptotic pathway was blocked by this vector (see below). Collectively, our results suggested that TG-induced apoptosis involved the DR5-mediated activation of caspase-8.

Confirmation of the RNAi Effect on Endogenous Genes—Prior to this study, we developed an algorithm for the identification of target sites using siRNA data sets obtained with reporter genes, such as genes for luciferases and green fluorescent protein (17). In this study, we examined whether or not the algorithm is applicable to endogenous genes. We constructed siRNA vectors directed against genes for *caspases 3*, *7*, *8*, and *9* and DR5, all of which might be involved in TG-induced apoptosis. As noted above, we used two different target sites per gene in these experiments. As shown in Fig. 2, Western blotting analysis indicated that the level of each respective protein was markedly reduced in cells that had been transfected with the siRNA vector targeted to the corresponding gene, whereas the control vector, targeted to the gene for the unrelated luciferase

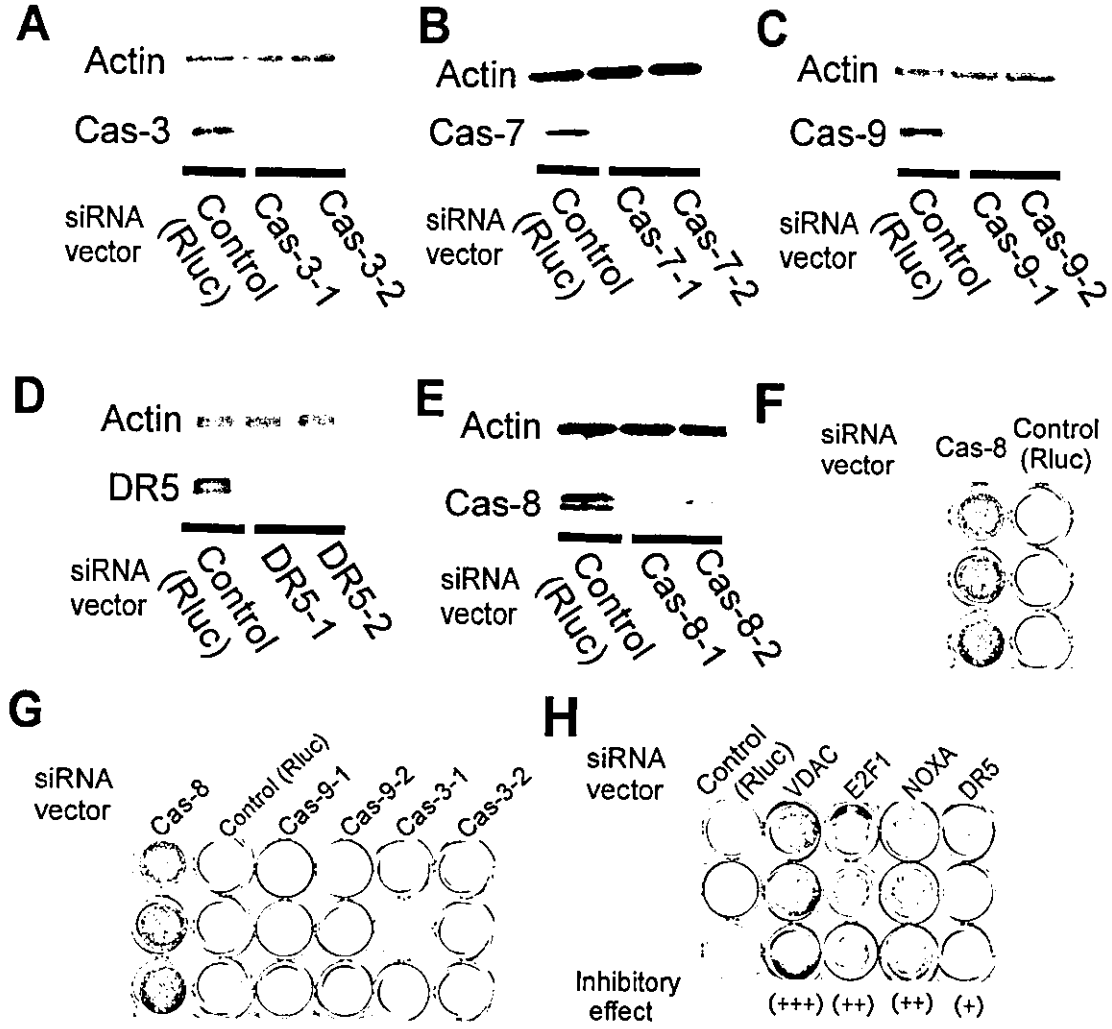

FIG. 2. **Confirmation of the RNAi effect on endogenous genes.** HCT116 cells were transfected with siRNA vectors directed against two target sites in the mRNA for caspase-3 (*A*), caspase-7 (*B*), caspase-9 (*C*), DR5 (*D*), caspase-8 (*E*), and *Renilla* luciferase (Rluc), as a control. *F–H*, surviving cells after treatment with TG and the indicated siRNA expression vector for 48 h. The living cells were stained with crystal violet. The results are representative of three independent experiments.

from *Renilla* (Rluc) had no effect. The levels of actin were unchanged, indicating that the effects of the siRNA vectors were specific to each respective gene (Fig. 2, *A–E*). These results suggested that our algorithm had allowed us to select appropriate sequences in endogenous genes (17). We also investigated the effects of siRNA vectors targeted to other genes by Western blotting. We confirmed that 70–80% of our siRNA vectors targeted to endogenous genes were able to silence these target genes very effectively.

Screening Strategy—We set the conditions for screening our siRNA expression library for the siRNAs that targeted genes involved in TG-induced apoptosis using an siRNA vector targeted to caspase-8 mRNA as a positive control. First, we investigated the duration of the effects of RNAi at the protein level after transfection of cells with this siRNA vector. To remove nontransfected cells, we treated cells with 2 μg/ml puromycin for 36–48 h and then analyzed levels of caspase-8. Reductions in levels of caspase-8 were sustained for at least 72–120 h after transfection, and inhibitory effects on apoptosis were observed over the same time range (Fig. 2*F* and data not shown). Under similar conditions, we used the siRNA expression library to screen for apoptosis-related genes. Thus, 36 h after transfection, we selected transfected cells by exposing cells to 2 μg/ml puromycin for 36 h. Then same number of cells were transferred in triplicate to a 96-well plate. After a further 12 h, we treated with 1 μM TG for another 48 h. Then we fixed the cells and stained them with crystal violet. Negative control cells that had been transfected with siRNA vectors targeting to Rluc and other unrelated transgenes were all dead by the treatment of TG (Fig. 2*F*, *right lane*). Under this condition, siRNA expression vector library was screened, and we selected siRNA vectors that made cells survive after treatment with TG. We identified the siRNA vectors specific for several genes that suppressed TG-induced apoptosis (Table I and Fig. 2*H*). Targeted genes were divided into three classes according to the extent of cell survival.

Caspases—The strong inhibitory effect of the siRNA vector for the gene directed against caspase-8 indicated that this enzyme is a key molecule in TG-induced apoptosis. Cells transfected with siRNA vectors directed against *DR5* mRNA resisted TG-induced apoptosis, but their survival was poorer than that of cells that had been transfected with siRNA vectors against the gene for *caspase-8*. In terms of protein levels, *DR5*-specific siRNA vectors almost completely suppressed the expression of *DR5* (Fig. 2*D*), suggesting the possible existence of a DR5-independent pathway(s) for activation of caspase-8 that involves other receptors (such as FAS and tumor necrosis factor α receptors) or, perhaps, of a receptor-independent caspase activation pathway(s).

The suppression caused by siRNA vectors directed against *Apaf1*, *VDAC*, and *Bid* indicated that the TG-induced apoptotic pathway also involved mitochondria. By contrast, the siRNA

TABLE I
List of targeted genes that promoted TG-induced apoptosis

Targeted gene	Accession number	Inhibitory effect of siRNA
Transcription factors		
E2F1	NM_005225	++
Caspases		
Caspase-8	NM_001228	+++
Members of the bcl-2 family		
Bad	NM_004322	+
Bid	NM_001196	+
PUMA	NM_014417	+
NOXA	NM_021127	++
MAPKs		
MAP3K8	NM_005204	++
MAP3K6	NM_004672	+
MAP3K3	NM_002401	+
MAP2K2	NM_030662	++
MAPK1	NM_002745	++
Others		
DR5	NM_003842	+
VDAC	NM_003374	+++
Apaf1	NM_001160	++

vectors targeted to genes for caspase-9 and caspase-3 failed to suppress TG-induced apoptosis (Fig. 2*G*) despite the almost complete suppression of the expression of these two genes (Fig. 2, *A* and C). However, siRNA vectors directed against genes for caspase-3 and caspase-9 did block apoptosis that was induced by stimuli other than TG (*e.g.* double-stranded RNA; data not shown). Although it has been proposed that both caspase-9 and Apaf1 are necessary for the activation of downstream caspases, Ho *et al.* (21) recently reported the presence of a caspase-9-dependent and Apaf1-independent apoptotic pathway in myoblast. Our data indicate that TG-induced apoptosis is dependent on Apaf1 but not on caspase-9 or on caspase-3, leading to the first identification, to our knowledge, of components of an apoptotic pathway downstream of mitochondria.

Bcl-2 and BH3-only Protein Families—The siRNA vectors targeted against the *Bad*, *PUMA*, and *NOXA* genes for the members of the Bcl-2 homology domain 3 family (the BH3-only protein family) inhibited TG-induced apoptosis. When pro-apoptotic members of the Bcl-2 family, such as Bax and Bak, are activated, they increase the permeability of the outer mitochondrial membrane and induce the release of pro-apoptotic proteins from the mitochondria. In normal cells, anti-apoptotic members of the Bcl-2 family, such as Bcl-2 and Bcl-xL, inhibit this activation and support cell survival. BH3-only proteins inhibit the actions of anti-apoptotic members of the Bcl-2 family and induce apoptosis. When levels of cytoplasmic Ca^{2+} ions rise, after treatment of cells with TG, Bad is activated and translocated to mitochondria (22). Thus, Bad might be a candidate for a messenger that conveys a signal from the ER to the mitochondria.

The siRNA vectors targeted against the *PUMA* and *NOXA* genes also inhibited TG-induced apoptosis. These genes induce apoptosis in response to DNA damage or to the overexpression of p53, but there are no reports that *NOXA* regulates ER stress-induced apoptosis. Moreover, Reimertz *et al.* (23) suggested that *PUMA* might be both sufficient and necessary for ER stress-induced apoptosis. To identify components of the apoptotic pathway downstream of the BH3-only proteins, we investigated the activation of the caspase cascade in cells that had been transfected with siRNA vectors directed against the gene for caspase-8, *NOXA*, and *PUMA* (Fig. 3). The siRNA vectors against *PUMA* or *NOXA* blocked the activation of caspase-9 but failed to prevent the processing of caspase-3 and Bid. These observations indicated that *NOXA* and *PUMA* act upstream of a mitochondrial pathway (an intrinsic pathway) but are not part of the extrinsic pathway that is initiated by

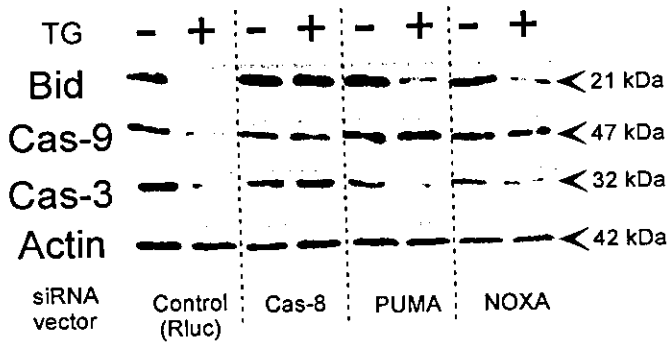

FIG. 3. **Characterization of the role of *PUMA* and *NOXA* in TG-induced apoptosis.** HCT116 cells were transfected with siRNA vectors directed against genes for caspase-8, PUMA, NOXA, and a negative control (Rluc). Eighty-four hours later, the cells were treated with TG for 24 h, and Western blotting analysis was performed with antibodies against the indicated proteins.

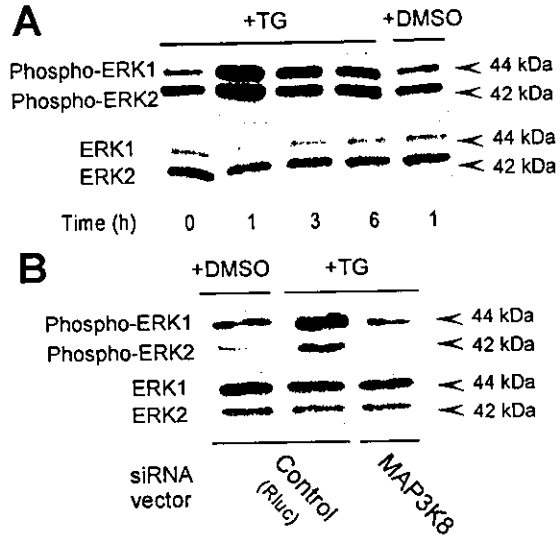

FIG. 4. **Suppression of genes for MAP3Ks inhibited the activation of ERK in TG-induced apoptosis.** *A*, HCT116 cells were treated with 1 μM TG or vehicle (dimethyl sulfoxide, *DMSO*) for the indicated times and analyzed by Western blotting with antibodies against the indicated proteins. *B*, the siRNA vector directed against the gene for *MAP3K8* suppressed the activation of the genes for ERK1/2.

activation of cell surface death receptors and subsequent direct cleavage of caspase-3 by caspase-8. By contrast, the siRNA vector directed against the gene for caspase-8 prevented the processing of Bid, caspase-9, and caspase-3, suggesting that caspase-8 might operate upstream of both the intrinsic pathway, presumably via activation of Bid (24), and the extrinsic pathway.

Numerous studies, including "knockout" experiments, have indicated that individual BH3-only proteins have specialized physiological roles. For example, Bim plays a role in the cytotoxic response of lymphocytes to cytokine deprivation and to taxol, whereas Bmf seems to be required for anoikis (apoptosis triggered by loss of contact with the extracellular matrix) (24). Our data demonstrated the involvement of several BH3-only proteins in the apoptotic pathway and showed that each of these BH3-only proteins is essential for the induction of apoptosis, suggesting the possible importance of the coordination of the activities of several BH3-only proteins in apoptosis.

Protein Kinases—Our screening revealed the involvement of members of the mitogen-activated protein kinase (MAPK) family in TG-induced apoptosis. MAPKs regulate the activity of transcription factors or downstream kinases by phosphorylation, thereby controlling a variety of physiological processes. MAPKs can be classified broadly into three categories: the

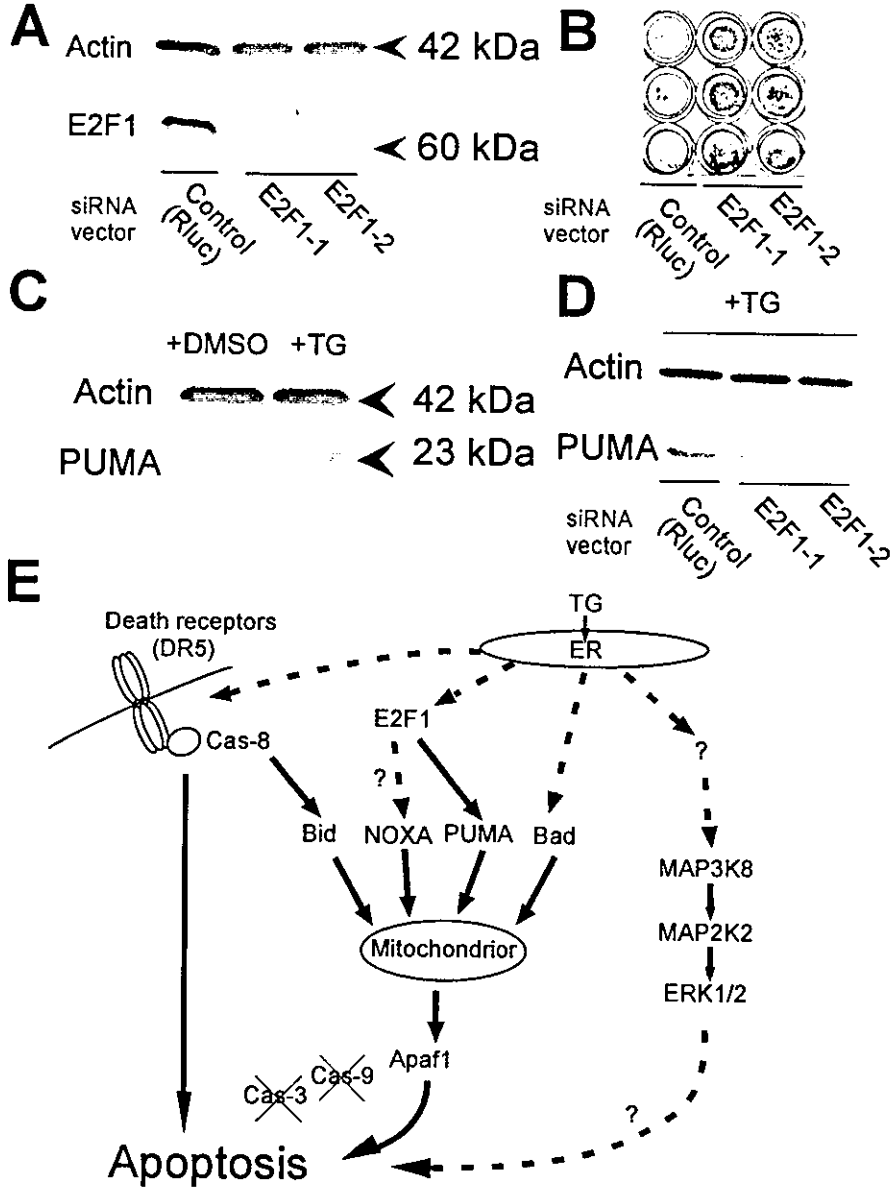

FIG. 5. **Suppression of expression of the *E2F1* gene blocked the enhancement of the expression of the *PUMA* gene in response to TG.** *A*, confirmation of the effects of siRNA vectors directed against the *E2F1* gene. HCT116 cells were transfected with siRNA vectors directed against two target sites in the *E2F1* gene (*lane 2*, siE2F1-1; *lane 3*, siE2F1-2), or with the siRNA vector directed against Rluc, as a control. During Western blotting analysis, the membranes were probed with antibodies against the indicated proteins. *B*, surviving cells after treatment with TG (1 μM) for 48 h. The cells were stained with crystal violet. *C*, expression of the *PUMA* gene was enhanced by TG. HCT116 cells were treated with 1 μM TG or vehicle (dimethyl sulfoxide, *DMSO*) for 36 h. During Western blotting analysis, the membranes were probed with antibodies against the indicated proteins. *D*, HCT116 cells transfected with siRNA vectors directed against *E2F1* gene were treated with 1 μM TG for 36 h. Western blotting of cell lysates was performed with antibodies against the indicated proteins. *E*, a model for TG-induced apoptosis.

ERKs, the c-Jun amino-terminal kinase (JNK), and the MAPK p38 (p38). In our screening, we identified siRNA vectors that targeted genes for ERK2 (MAPK1), MAP2K2, and MAP3Ks (MAP3K3, MAP3K6, and MAP3K8), and we identified these genes as genes that might be involved in TG-induced apoptosis (Table I).

To confirm the involvement of the ERK pathway in TG-induced apoptosis, we examined the activation of ERK1/ERK2 by Western blotting with a phospho-ERK-specific antibody. As shown in Fig. 4*A*, ERK1/ERK2 was activated 1 h after the start of treatment of cells with TG. Furthermore, suppression of the expression of MAP3K8 clearly impaired the activation of ERK after the start of treatment with TG (Fig. 4*B*). Although the activation of the ERK and JNK/p38 cascades are generally considered to participate in survival and in stress/death signaling, respectively (25), we failed to detect the involvement of JNK/p38 in TG-induced apoptosis in our screening, even though some siRNA vectors targeted to *JNK* and *p38* were identified as anti-apoptotic siRNAs in our screening for genes in other apoptotic pathways.[2] Collectively, our results suggest that the activity of ERKs, mediated by MAP3K8, but probably not JNK/p38, might play a pro-apoptotic role in TG-induced apoptosis.

Transcription Factors—An siRNA vector directed against *E2F1* also acted as a suppressor of TG-induced apoptosis (Fig. 5, *A* and *B*). E2F1, a member of the E2F family of transcription factors, is known for its involvement of DNA replication during cell proliferation. E2F1 also regulates apoptosis, and a number of E2F1-regulated genes, including genes for ARF, p73, Apaf1, and BH3-only proteins, participate in apoptosis (26–29). The expression of E2F1 is enhanced and E2F1 induces apoptosis in response to DNA damage (30). It seems possible that suppression of the expression of *E2F1* might result in the blockage of TG-induced apoptosis. Hershko and Ginsberg (29) showed that ectopic expression of E2F1 enhanced the expression of the pro-apoptotic BH3-only protein PUMA via direct involvement in transcription in NIH3T3 cells.

As noted above, siRNA vectors directed against *PUMA* suppressed TG-induced apoptosis, and E2F1 appeared to regulate TG-induced apoptosis via regulation of the expression of *PUMA*. Reimertz *et al.* (23) demonstrated that significant induction of PUMA in response to TG, and our Western blotting analysis demonstrated that enhancement of the expression of *PUMA* occurred after treatment of cells with TG (Fig. 5*C*). This

[2] S. Matsumoto, M. Miyagishi, H. Akashi, R. Nagai, and K. Taira, unpublished data.

enhancement was not observed in cells in which the expression of *PUMA* was suppressed via the siRNA vector directed against *E2F1* (Fig. 5*D*). These results suggest that endogenous E2F1 might regulate TG-induced apoptosis via regulation of the expression of *PUMA*.

DISCUSSION

The data presented here, together with those from other studies (31), suggest a model for TG-induced apoptosis, as shown in Fig. 5*E*. By screening our siRNA expression library, we were able to identify some novel pathways in TG-induced apoptosis in HCT116 cells. We first detected the death receptor/caspase-8 pathway, which seems to induce both the mitochondrial pathway via cleavage of Bid, and the extrinsic pathway, which bypasses the mitochondrial pathway. We also observed the involvement of three BH3 proteins, which might induce the mitochondrial pathway. Transcription factors in the E2F family appeared to enhance the expression of *PUMA*. The ERK pathway, which was activated transiently 1 h after the start of treatment with TG and is mediated by MAP3K8, might be part of the TG-induced apoptotic pathway. In preliminary experiments, designed to determine hierarchical relationships among these pathways, we found that the ERK pathway does not appear to be located upstream of the death receptor/caspase-8 pathway and the mitochondrial pathway, and it seems likely that the ERK pathway functions as an independent pathway (data not shown).

The most significant advantages of our siRNA expression library as compared with the widely used synthetic siRNA library are as follows. The interferon response in transfected cells can be avoided (32), and the RNAi effect is sustained for a longer period of time than the inhibitory effects of synthetic siRNAs, in particular in proliferating cells. Using our siRNA expression library, we demonstrated here the straightforward identification of novel pathways that had not been identified by other available strategies. We have already constructed siRNA libraries directed against the genes for all the kinases and phosphatases in the human genome and against other genes as well. Further analyses using our large libraries of siRNA expression vectors should provide more precise information about various signaling pathways and enhance our understanding of numerous physiological phenomena.

REFERENCES

1. Dykxhoorn, D. M., Novina, C. D., and Sharp, P. A. (2003) *Nat. Rev. Mol. Cell. Biol.* **6**, 457–467
2. Fire, A., Xu, S., Montgomery, M. K., Kostas, S. A., Driver, S. E., and Mello, C. C. (1998) *Nature* **391**, 806–811
3. Fraser, A. G., Kamath, R. S., Zipperlen, P., Martinez-Campos, M., Sohrmann, M., and Ahringer, J. (2000) *Nature* **408**, 325–330
4. Gonczy, P., Echevern, C. Oegema, K. Coulson, A., Jones, S. J., Copley, R. R., Duperon, J., Oegema, J., Brehm, M., Cassin, E., E., Hannak, E., Kirkham, M., Pichler, S., Flohrs, K., Goessen, A., Leidel, S., Alleaume, A. M., Martin, C., Ozlu, N., Bork, P., and Hyman, A. A. (2000). *Nature* **408**, 331–336
5. Lee, S. S., Lee, R. Y., Fraser, A. G., Kamath, R. S., Ahringer, J., Ruvkun, G., and Choi, K. Y. (2003) *Nat. Genet.* **33**, 40–48
6. Pothof, J., van Haaften, G., Thijssen, K., Kamath, R. S., Fraser, A. G., Ahringer, J., Plasterk, R. H., Tijsterman, M., and Simmer, F. (2003) *Genes Dev.* **17**, 443–448
7. Stark, G. R., Kerr, I. M., Williams, B. R., Silverman, R. H., and Schreiber, R. D. (1998) *Annu. Rev. Biochem.* **67**, 227–264
8. Elbashir, S. M., Harborth, J., Lendeckel, W., Yalcin, A., Weber, K., and Tuschl, T. (2001) *Nature* **6836**, 494–498
9. Brummelkamp, T. R., Bernards, R., and Agami, R. (2002) *Science* **296**, 550–553
10. Miyagishi, M., and Taira, K. (2002) *Nat. Biotechnol.* **20**, 497–500
11. Paddison, P. J., Caudy, A. A., Bernstein, E., Hannon, G. J., and Conklin, D. S. (2002) *Genes Dev.* **16**, 948–958
12. Lee, N. S., Dohjima, T., Bauer, G., Li, H., Li, M. J., Ehsani, A., Salvaterra, P., and Rossi, J. (2002) *Nat. Biotechnol.* **20**, 500–505
13. Sui, G., Soohoo, C., Affar, el B., Gay, F., Shi, Y., Forrester, W. C., and Shi, Y. (2002) *Proc. Natl. Acad. Sci. U. S. A.* **99**, 5515–5520
14. Paul, C. P., Good, P. D., Winer, I., and Engelke, D. R. (2002) *Nat. Biotechnol.* **20**, 505–508
15. Yu, J. Y., DeRuiter, S. L., and Turner, D. L. (2002) *Proc. Natl. Acad. Sci. U. S. A.* **99**, 6047–6052
16. Kawasaki, H., and Taira, K. (2003) *Nucleic Acids Res.* **31**, 700–707
17. Miyagishi, M., and Taira, K. (2003) *Oligonucleotides* **13**, 325–333
18. Futami, T., Miyagishi, M., Iwai, S., Seki, M., and Taira, K. (2003) *Antisense Nucleic Acid Drug Dev.* **13**, 9–17
19. Jackson, A. L., Bartz, S. R., Schelter, J., Kobayashi, S. V., Burchard, J., Mao, M., Li, B., Cavet, G., and Linsley, P. S. (2003) *Nat. Biotechnol.* **21**, 635–637
20. He, Q., Montalbano, J., Corcoran, C., Jin, W., Huang, Y., and Sheikh, M. S. (2003) *Oncogene* **22**, 2674–2679
21. Ho, A. T., Li, Q. H., Hakem, R., Mak, T. W., and Zacksenhaus, E. (2004) *EMBO J.* **23**, 460–472
22. Wang, H. G., Pathan, N., Ethell, I. M., Krajewski, S., Yamaguchi, Y., Shibasaki, F., McKeon, F., Bobo, T., Franke, T. F., and Reed, J. C. (1999) *Science* **284**, 339–343
23. Reimertz, C., Kogel, D., Rami, A., Chittenden, T., and Prehn, J. H. (2003) *J. Cell Biol.* **162**, 587–597
24. Cory, S., and Adams, J. M. (2002) *Nat. Rev. Cancer* **2**, 647–656
25. Murray, B., Alessandrini, A., Cole, A. J., Yee, A. G., and Furshpan, E. J. (1998) *Proc. Natl. Acad. Sci. U. S. A.* **95**, 11975–11980
26. Muller, H., Bracken, A. P., Vernell, R., Moroni, M. C., Christians, F., Grassilli, E., Prosperini, E., Vigo, E., Oliner, J. D., and Helin, K. (2001) *Genes Dev.* **15**, 267–285
27. Stanelle J, Stiewe, T., Theseling, C. C., Peter, M., and Putzer, B. M. (2002) *Nucleic Acids Res.* **30**, 1859–1867
28. Nahle, Z., Polakoff, J., Davuluri, R. V., McCurrach, M. E., Jacobson, M. D., Narita, M., Zhang, M. Q., Lazebnik, Y., Bar-Sagi, D., and Lowe, S. W. (2002) *Nat. Cell Biol.* **11**, 859–864
29. Hershko, T., and Ginsberg, D. (2004) *J. Biol. Chem.* **279**, 8627–8634
30. Pediconi, N., Ianari, A., Costanzo, A., Belloni, L., Gallo, R., Cimino, L., Porcellini, A., Screpanti, I., Balsano, C., Alesse, E., Gulino, A., and Levrero, M. (2003) *Nat. Cell Biol.* **5**, 552–558
31. Rutkowski, D. T., and Kaufman, R. J. (2004) *Trends Cell Biol.* **4**, 20–28
32. Miyagishi, M., Matsumoto, M., Futami, T., Akashi, H., Appasani, K., Takagi, Y., Sutou, S., Kadowaki, T., Nagai, R., and Taira, K. (2005) in *RNA Interference Technology* (Appasani, K., ed) Cambridge University Press, in press

nature immunology

The RNA helicase RIG-I has an essential function in double-stranded RNA-induced innate antiviral responses

Mitsutoshi Yoneyama[1], Mika Kikuchi[1], Takashi Natsukawa[1], Noriaki Shinobu[1], Tadaatsu Imaizumi[2], Makoto Miyagishi[3], Kazunari Taira[3], Shizuo Akira[4] & Takashi Fujita[1]

Intracellular double-stranded RNA (dsRNA) is a chief sign of replication for many viruses. Host mechanisms detect the dsRNA and initiate antiviral responses. In this report, we identify retinoic acid inducible gene I (RIG-I), which encodes a DExD/H box RNA helicase that contains a caspase recruitment domain, as an essential regulator for dsRNA-induced signaling, as assessed by functional screening and assays. A helicase domain with intact ATPase activity was responsible for the dsRNA-mediated signaling. The caspase recruitment domain transmitted 'downstream' signals, resulting in the activation of transcription factors NF-κB and IRF-3. Subsequent gene activation by these factors induced antiviral functions, including type I interferon production. Thus, RIG-I is key in the detection and subsequent eradication of the replicating viral genomes.

Type I interferon (IFN), which comprises IFN-β and the IFN-α family, is central in the antiviral innate immunity of mammals and also has a preparatory function for the subsequent adaptive immunity[1–3]. The expression of type I interferon is strictly regulated by the activation of pre-existing transcription factors, such as interferon regulatory factor 3 (IRF-3)[4–8], nuclear factor-κB (NF-κB)[9–11] and ATF-2–c-Jun[12]. An essential function for IRF-3 was demonstrated by analysis of IRF-3-deficient cells[13]. After viral infection of cells, IRF-3, which is normally in the cytoplasm, is immediately phosphorylated at specific serine residues in its C-terminal regulatory domain. It then dimerizes and translocates to the nucleus. The dimerized IRF-3 interacts with the transcriptional coactivator p300 or CREB-binding protein in the nucleus, resulting in specific DNA-binding activity[4–8,14]. Two members of the inhibitor of NF-κB (IκB) kinase (IKK) family, TANK-binding kinase 1 (TBK1) and IKK-i (also known as IKKε), have been identified as potential activators for IRF-3 (refs. 15,16). These kinases directly phosphorylate the C-terminal serine residues of IRF-3 (ref. 17). However, their regulatory mechanisms are still unknown.

Type I interferon is induced by bacterial components such as lipopolysaccharide and CpG DNA in leukocytes, such as macrophages and dendritic cells[18,19], as well as by viral infection. Targeted gene-disruption studies have shown that Toll-like receptors (TLRs) recognize pathogen-associated molecular patterns. TLR3, TLR4, mouse TLR7 (TLR8, for humans) and TLR9 function as signaling receptors for extracellular double-stranded RNA (dsRNA)[20], lipopolysaccharide[21,22], viral single-stranded RNA[23–25] and CpG DNA[26], respectively. The interaction of these pathogen-associated molecular patterns with the extracellular leucine-rich repeat of the TLR facilitates the recruitment of adaptor molecules to the cytoplasmic Toll–interleukin 1 receptor domain of the TLR. Adaptors MyD88, IRAK and TRAF6 are recruited by many TLRs and activate signaling cascades[27]. For TLR7 and TLR9, type I interferon is induced by this MyD88-dependent pathway[25,28]; however, the precise mechanism of this pathway has been poorly characterized. TLR4 and TLR3 activate additional signaling pathway called the MyD88-independent pathway, which recruits another adaptor molecule, Trif (also known as TICAM-1), and activates a second set of genes, including those of type I interferon, through activation of IRF-3 (refs. 29–32). Trif has the potential to associate directly with IKK-i and TBK1 (ref. 15).

For most types of cells it has been postulated that the replication of viruses results in an accumulation of intracellular dsRNA, which triggers host response mechanisms that include expression of type I interferon. This signaling pathway is apparently distinct from that mediated by TLR3 (ref. 33) and constitutes a chief pathway activated by viral infection. No evidence at present, however, supports the idea that dsRNA-dependent protein kinase or its activator or 2′-5′ oligoadenylate synthase are involved[33–35].

[1]Department of Tumor Cell Biology, Tokyo Metropolitan Institute of Medical Science, Tokyo Metropolitan Organization for Medical Research, 3-18-22 Honkomagome, Bunkyo-ku, Tokyo 113-8613, Japan. [2]Department of Vascular Biology, Hirosaki University School of Medicine, 5 Zaifu-cho, Hirosaki 036-8562, Japan. [3]Department of Chemistry and Biotechnology, School of Engineering, University of Tokyo, Hongo, Bunkyo-ku, Tokyo 113-8656, Japan. [4]Department of Host Defense, Research Institute for Microbial Diseases, Osaka University, 3-1 Yamada-oka, Suita, Osaka 565-0871, Japan. Correspondence should be addressed to T.F. (fujita@rinshoken.or.jp).

Published online 20 June 2004; doi:10.1038/ni1087

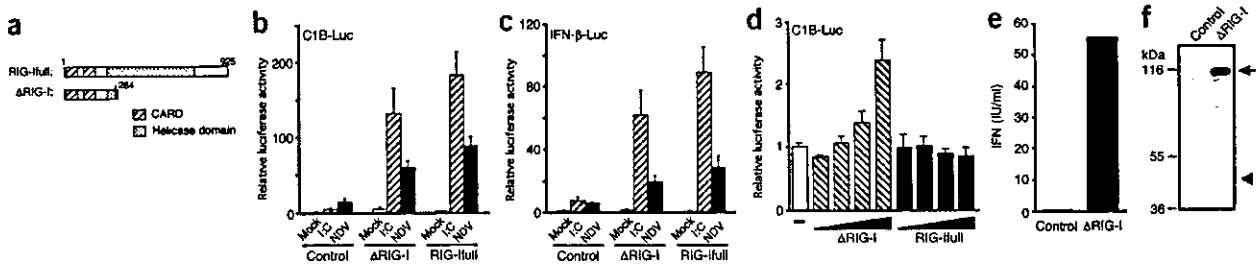

Figure 1 Identification of the CARD of RIG-I as a positive regulator for type I interferon. (**a**) RIG-I constructs, including the CARD and helicase domain. ΔRIG-I contains an additional 22 amino acids derived from the vector sequence (filled box). (**b**,**c**) L929 cells were transiently transfected with reporter constructs containing repeated IRF-binding sites (p-55C1BLuc; C1B-Luc; **b**) or the natural IFN-β promoter (p-125Luc; IFN-β-Luc; **c**) together with empty vector pEF-BOS (Control), ΔRIG-I or RIG-Ifull. The reporter/effecter ratio was 1:1. As an internal control, a *Renilla* luciferase construct was transfected with each of the three. Transfected cells were mock treated (Mock), transfected with poly(I:C) for 6 h (I:C) or treated with NDV for 12 h (NDV) and were subjected to the Dual-Luciferase assay. Data represent relative firefly luciferase activity, normalized to *Renilla* luciferase activity; error bars show s.d. of triplicate transfections. (**d**) Constitutive activity of p-55C1BLuc determined as described in **b**, except that the reporter/effecter ratio was varied (1:0.2, 1:0.4, 1:0.6 and 1:0.8; wedges) or without effector (–). (**e**,**f**) 293T cells were transfected with control vector or ΔRIG-I. (**e**) IFN-β in culture medium was quantified by ELISA. (**f**) Cell lysates were separated by SDS-PAGE and probed with anti-RIG-I; transfected ΔRIG-I (arrowhead) and endogenous RIG-I (arrow) were detected. Data are representative of two independent experiments.

Here we demonstrate that the DExD/H box–containing RNA helicase retinoic acid inducible gene I (RIG-I) is important in virus-induced activation of type I interferon. The DExD/H box RNA helicases, defined by their ability to unwind dsRNA with their intrinsic ATPase activity, are found in almost all organisms from viruses to mammals and are involved in many important processes, including RNA interference (RNAi)[36,37]. RIG-I has an interesting structural feature: it has two copies of a caspase recruitment domain (CARD) at its N terminus in addition to its C-terminal helicase domain[38,39]. We provide several lines of evidence to show that the CARD of RIG-I transduces signals that lead to the activation of IRF-3 and NF-κB. Full-length RIG-I can interact with dsRNA and augment interferon production in response to viral infection in an ATPase-dependent way. These results suggest that RIG-I functions as an essential regulator for virus-induced antiviral immunity.

RESULTS

Activation of interferon promoter by the CARD of RIG-I

To identify the molecule(s) involved in intracellular dsRNA-induced expression of interferon, we generated an expression cDNA library from IFN-β-treated human K562 cells, which lack the entire locus encoding multiple type I interferon molecules. We chose this library based on our observation that K562 cells do not activate IRF-3 after virus infection; however, this hyporesponsiveness can be overcome by IFN-β pre-treatment (**Supplementary Fig. 1** online). We transfected the RNA duplex poly(rI):poly(rC) (poly(I:C)) into mouse L929 cells to induce a reporter regulated by repeated IRF-binding sites (p-55C1BLuc), and screened the library for its ability to enhance expression of this reporter. Of 1×10^5 cDNAs, we isolated one clone that notably enhanced the induction by dsRNA transfection. The clone seemed to encode N-terminal residues of the DExD/H box helicase RIG-I (ΔRIG-I; **Fig. 1a**). Full-length RIG-I consists of a helicase domain and tandem CARD motifs. As ΔRIG-I encompassed two copies of CARD but was devoid of the helicase domain, we also constructed expression vector for full-length RIG-I (RIG-Ifull) and examined the activities of these constructs. Expression of either protein enhanced the induction of p-55C1BLuc after either dsRNA transfection or infection of L929 cells with Newcastle disease virus (NDV; **Fig. 1b**). Expression of RIG-Ifull or ΔRIG-I did not affect expression of a reporter gene linked to a control thymidine kinase gene promoter (data not shown). The enhancement by NDV was less prominent, presumably because of partial suppression of virus replication by RIG-I (discussed below). We obtained essentially the same result when we used the reporter gene linked to the natural IFN-β promoter (p-125Luc; **Fig. 1c**). These results indicate that RIG-I was involved in dsRNA-induced activation of *IFNB1*. Expression of ΔRIG-I but not RIG-Ifull enhanced the basal activity of p-55C1BLuc in a dose-dependent way (**Fig. 1d**). Consistent with that result, endogenous IFN-β was secreted into the culture medium of human 293T cells after transient expression of ΔRIG-I (**Fig. 1e**). These results suggest that ectopic expression of the CARD of RIG-I can partially bypass dsRNA-induced signaling. At the same time, we noted the induction of endogenous RIG-I in cells expressing ΔRIG-I (**Fig. 1f**). As the gene encoding RIG-I is interferon inducible[40] (**Supplementary Fig. 1** online), this is probably because of autocrine interferon production, and the induced full-length RIG-I may be responsible for the activation of the interferon promoter after stimulation.

Activation of IRF-3 and NF-κB by ΔRIG-I

Activation of IRF-3 is essential for primary induction of type I interferon[13]. To test whether the RIG-I CARD activates IRF-3, we transfected a fusion protein of IRF-3 and the Gal4 DNA-binding domain along with either control vector or the ΔRIG-I expression vector into L929 cells. The reporter gene, regulated by the Gal4 upstream activation sequence, was activated by expression of ΔRIG-I, and the activation was moderately augmented by transfection of dsRNA (**Fig. 2a**). We do not know the reason for the poor inducibility by poly I:C or NDV in cells expressing ΔRIG-I. One possible explanation is that the activation by ΔRIG-I was saturated because of high intracellular accumulation of the Gal4–IRF-3 fusion (data not shown). Next, we examined IRF-3 dimerization. When we 'tagged' IRF-3 with an epitope of peptides derived from the p50 subunit of NF-κB[8] and transfected this together with ΔRIG-I into L929 cells, we detected the constitutive formation of the IRF-3-dimer and its further augmentation by dsRNA (**Fig. 2b**), consistent with the results of the reporter assay (**Fig. 1b**). In addition, we also noted DNA-binding activity, which involves the IRF-3-dimer and p300 or CREB-binding protein, in 293T cells expressing ΔRIG-I (**Fig. 2c**, left), approximately consistent with the results of the reporter assay using L929 cells (**Fig. 1b**). These data indicate that ΔRIG-I activates a signaling pathway leading to activation of IRF-3.

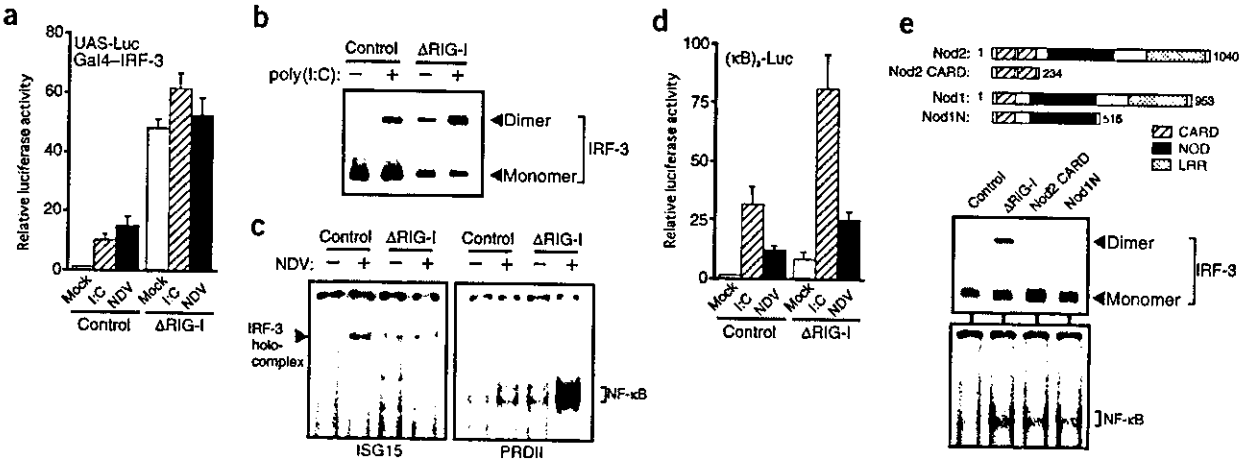

Figure 2 The RIG-I CARD constitutively activates both IRF-3 and NF-κB. (**a**) L929 cells were transfected with the reporter and the effector plasmids p-55UAS$_6$Luc (UAS-Luc) and pEFGal4–IRF-3 (Gal4–IRF-3) together with empty vector (Control) or ΔRIG-I. Luciferase activity was normalized to the internal control. Error bars represent s.d. of triplicate transfections. (**b**) IRF-3 tagged with the p50 epitope was transiently expressed in L929 cells with control or ΔRIG-I plasmid. After stimulation by poly(I:C) transfection for 6 h, lysates were separated by native PAGE and monomeric or dimerized IRF-3 (right margin) was detected by immunoblot with anti-p50. (**c**) 293T cells were transfected with p50-tagged IRF-3 and either control vector or ΔRIG-I plasmid, then were mock treated (–) or were infected with NDV for 9 h (+). Extracts were subjected to EMSA with ^{32}P-labeled oligonucleotides containing the IRF-binding sequence of the ISG15 promoter (left) or the NF-κB-binding site of *IFNB1* (PRDII; right) as probes. (**d**) The reporter construct regulated by the NF-κB-binding site (p-55A2Luc; (κB)$_3$-Luc) was transfected together with control vector or ΔRIG-I. Luciferase activity was determined as described in **a**. (**e**) Nod1, Nod2 and mutant proteins (top). NOD, nucleotide-binding oligomerization domain; LRR, leucine-rich repeat; Nod1N, truncated Nod1. p50-tagged IRF-3 expressed with proteins (above lanes) in 293T cells was detected by native PAGE followed by immunoblot (middle). Portions of the lysates were subjected to EMSA with NF-κB oligonucleotide as probe (bottom).

Because NF-κB is also activated by virus-induced signaling and participates in IFN-β expression[9–11], we tested the effect of ΔRIG-I on NF-κB activation. Expression of ΔRIG-I resulted in activation of a reporter gene containing NF-κB-binding sites (**Fig. 2d**). Again, this activation was further enhanced by induction by transfection of dsRNA or by viral infection. Also, in 293T cells expressing ΔRIG-I, we noted constitutive NF-κB DNA-binding activity as well as its enhancement by viral stimulation (**Fig. 2c**, right), consistent with the results of the reporter assay (**Fig. 2d**). These data suggest that ΔRIG-I can activate both IRF-3 and NF-κB, leading to constitutive expression of type I interferon.

The CARD is found in other signaling molecules, such as Nod1 and Nod2, which are linked to the signaling triggered by cytoplasmic pathogen-associated molecular patterns[41]. Notably, Nod2 contains a tandem CARD, similar to RIG-I (ref. 42). The CARDs of RIG-I, Nod1 and Nod2 all activated NF-κB; however, IRF-3 activation was induced only by the CARD of RIG-I, suggesting a divergence of common and specific signaling (**Fig. 2e**). We conclude therefore that the observed activity inducing IRF-3 was specific to the CARD of RIG-I.

Function of the helicase domain in signaling

The observation that overexpression of ΔRIG-I, which does not have C-terminal helicase domain, resulted in constitutive activation of the signal, led us to hypothesize that the CARD acts as an effector domain activating a downstream molecule. Although expression of RIG-Ifull also resulted in enhanced gene induction after transfection of dsRNA or viral infection, we found no basal activity, in contrast to results with ΔRIG-I (**Fig. 1d**). Furthermore, treatment of cells with type I interferon increased the amount of endogenous RIG-I (ref. 40; **Supplementary Fig. 1** online), but interferon treatment does not trigger the activation of interferon expression[43]. These observations suggest that the C-terminal helicase domain of RIG-I contains a regulatory function for signal transduction. To analyze the function of the helicase domain, we constructed an expression vector encoding only the helicase domain of RIG-I (RIG-IC; **Fig. 3a**). As a control we used eIF-4A, a DExD/H box RNA helicase distantly related to RIG-I. Although the RIG-Ifull augmented the reporter gene induction after infection of NDV, RIG-IC blocked virus-induced activation of the reporter (**Fig. 3b**) without inhibition of viral replication in infected cells (data not shown). We also found this dominant negative effect in L929 cells stimulated by dsRNA transfection (**Supplementary Fig. 2** online). Expression of eIF-4A produced neither a positive nor a negative effect on the reporter induction (**Fig. 3b**). To further address the function of the helicase domain of RIG-I, we introduced an empirical inactivating point mutation at the Walker-type ATP-binding site[44] using the full-length protein as the template (**Fig. 3a**). Reporter gene analysis again showed that the mutation inhibited the ability of RIG-I to accelerate virus-induced reporter activation and conferred dominant negative activity to RIG-I (**Fig. 3b**). These results suggest that the helicase activity of RIG-I was indispensable for these molecules to function as signal transducers.

The ATPase activity of DExD/H box RNA helicases is dsRNA dependent[36] and RIG-I was located exclusively in cytoplasm (unpublished data). Therefore, we speculated that RIG-I directly interacts with dsRNA in the cytoplasm and that this recognition acts as direct trigger of the signaling cascade. To examine the interaction with dsRNA, we produced RIG-I in 293T cells and subjected it to a poly(I:C)-agarose 'pulldown' assay. We detected interaction between poly(I:C) and RIG-I (**Fig. 3c**). To address the recognition specificity of RIG-I, we did a competition assay. RIG-I specifically recognized poly(I:C) and poly(rA):poly(rU), with relative preference for the former, but we found no substantial competition with single-stranded RNA (poly(A)) and dsDNA (**Fig. 3d**).

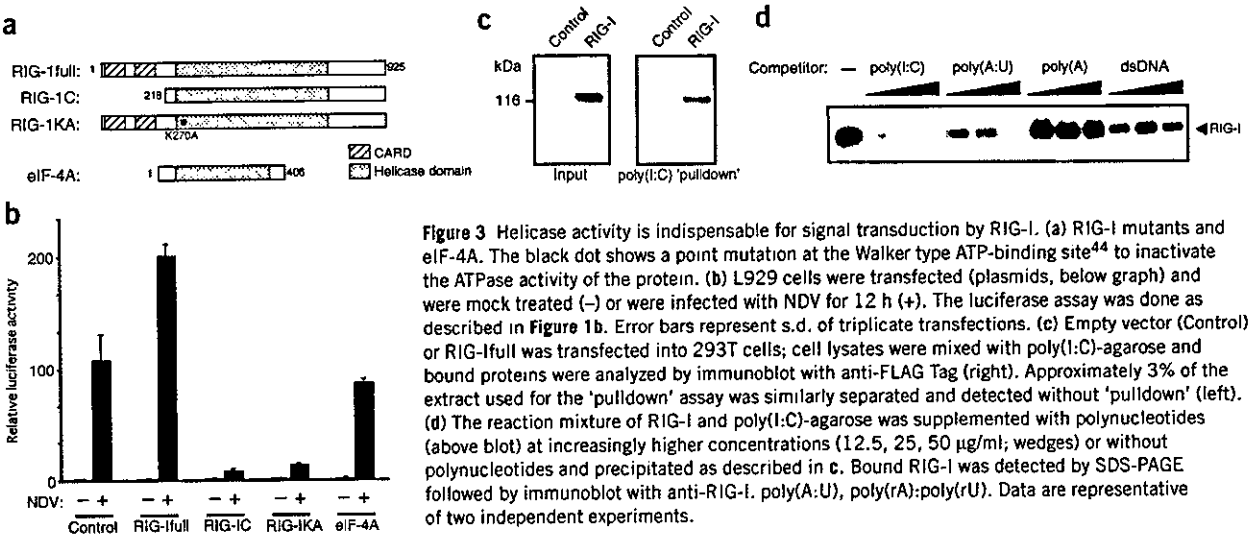

Figure 3 Helicase activity is indispensable for signal transduction by RIG-I. (**a**) RIG-I mutants and eIF-4A. The black dot shows a point mutation at the Walker type ATP-binding site[44] to inactivate the ATPase activity of the protein. (**b**) L929 cells were transfected (plasmids, below graph) and were mock treated (–) or were infected with NDV for 12 h (+). The luciferase assay was done as described in **Figure 1b**. Error bars represent s.d. of triplicate transfections. (**c**) Empty vector (Control) or RIG-Ifull was transfected into 293T cells; cell lysates were mixed with poly(I:C)-agarose and bound proteins were analyzed by immunoblot with anti-FLAG Tag (right). Approximately 3% of the extract used for the 'pulldown' assay was similarly separated and detected without 'pulldown' (left). (**d**) The reaction mixture of RIG-I and poly(I:C)-agarose was supplemented with polynucleotides (above blot) at increasingly higher concentrations (12.5, 25, 50 μg/ml; wedges) or without polynucleotides and precipitated as described in **c**. Bound RIG-I was detected by SDS-PAGE followed by immunoblot with anti-RIG-I. poly(A:U), poly(rA):poly(rU). Data are representative of two independent experiments.

RIG-I is essential for virus-induced gene expression

To investigate the function of RIG-I in signal transduction in cells, we used the RNAi technique to inhibit endogenous expression of RIG-I. Expression of small interfering RNA (siRNA) for mouse RIG-I mRNA, but not control siRNA, inhibited expression of endogenous RIG-I in mouse L929 cells (**Fig. 4a**). In these cells, activation of endogenous IRF-3 after viral infection was impaired (**Fig. 4b**). Furthermore, quantitative RT-PCR experiment showed that virus-induced expression of type I interferon (*Ifna4* and *Ifnb*), *Cxcl10* (encoding the chemokine IP-10) and *Ccl5* (encoding the chemokine RANTES) was also inhibited (**Fig. 4c**). The inhibition of gene induction, particularly of *Ifna4* and *Ifnb*, was substantial compared with the suppression of RIG-I protein by RNAi. This result was presumably because of the autoamplification property of RIG-I expression; that is, low abundance of RIG-I uncouples the amplification loop through autocrine type I interferon, resulting in considerable impairment of *Ifn* gene induction. These results indicate that RIG-I is essential in virus-induced expression of genes associated with innate antiviral responses.

Reduction in viral yield by RIG-I

The results described above indicate that expression of full-length RIG-I sensitized cells to respond after viral infection to activate a set of genes including *Ifn* and interferon-responsive genes. We speculated, therefore, that increased expression of full-length RIG-I can confer antiviral activity directly as well as indirectly by activating the interferon system. To address this, we challenged a stable L929 cell transformant expressing RIG-Ifull and control transformant with vesicular stomatitis virus (VSV) (**Fig. 5a**) or encephalomyocarditis virus (EMCV; **Fig. 5b**) at various multiplicities of infection (MOI). Control cells showed cytopathic effect after infection of the viruses at all MOI tested (**Fig. 5b**, top left). However, RIG-Ifull transformant cells showed less-severe pathology (**Fig. 5b**, top right). In agreement with this result, viral yield was reduced by two to three logs in the RIG-Ifull transformant for either virus (**Fig. 5b**, bottom). This protection was not because of constitutive production of antiviral humoral factors such as type I interferon in the culture supernatant, as conditioned medium of the uninfected RIG-Ifull transformant failed to confer antiviral activity to fresh L929 cells (data not shown). Furthermore, RIG-I suppressed a single round of viral replication in the presence of neutralizing antibody to type I interferon (anti-type I interferon; **Supplementary Fig. 3** online). These results demonstrate that RIG-I exerts an antiviral effect directly, at least at the early in the infection cycle. These data emphasize the biological relevance of RIG-I in antiviral innate immunity.

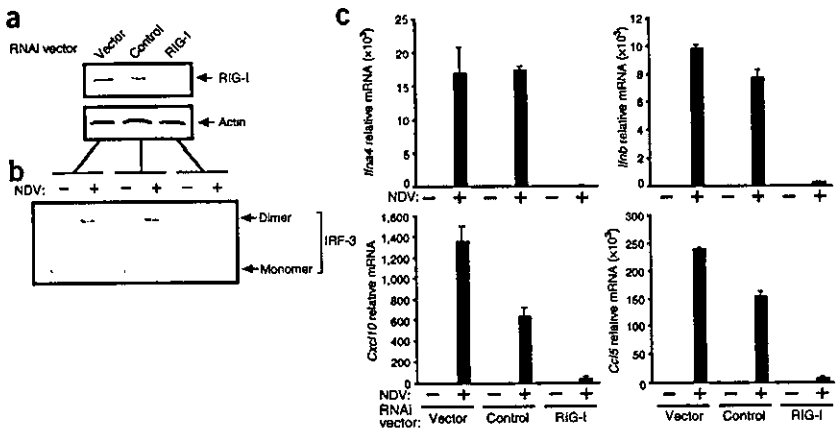

Figure 4 RIG-I is required for activation of IRF-3 and virus-induced gene expression. L929 cells transfected with RNAi vector alone (Vector), vector for nonspecific siRNA (Control) or vector for siRNA targeting mouse RIG-I (RIG-I) were mock-infected (–) or were infected with NDV for 9 h (+). (**a**) Endogenous RIG-I or actin in uninfected cells monitored by SDS-PAGE followed by immunoblot. (**b**) Activation of IRF-3 assessed by native PAGE followed by immunoblot. (**c**) Expression of *Ifna4*, *Ifnb*, *Cxc10* and *Ccl5* detected by real-time PCR. Data were normalized to the abundance of internal 18S rRNA. These results were reproducibly obtained in two independent transfection experiments. Error bars indicate triplicate samples of experiments.

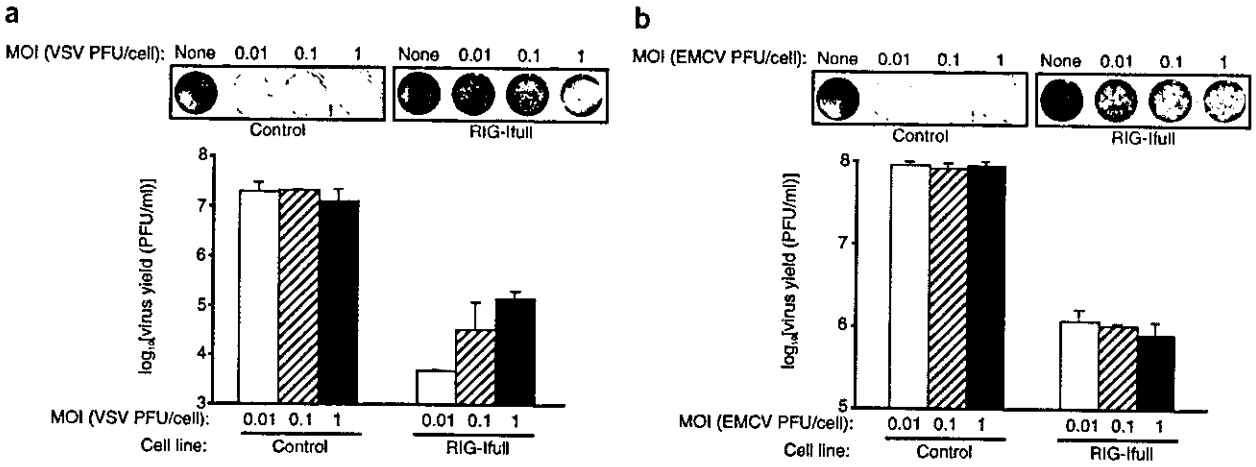

Figure 5 Reduction in viral yield by RIG-I. L929-derived stable transformants by empty vector (Control) or RIG-Ifull were infected with VSV (a) or EMCV (b) at the indicated MOI. After 24 h of infection, cells were stained with amido black (top). Virus yield in the supernatant at 24 h after infection was determined by plaque assay (bottom). The same results were reproducibly obtained in two independent experiments (**Supplementary Fig. 3** online). Error bars indicate triplicate samples of experiments. PFU, plaque-forming unit.

RIG-I-mediated signaling and other signaling pathways

Viral infection or transfection of poly(I:C) leads to activation of IRF-3 and subsequent gene induction in the presence or absence of functional *Tlr3* (ref. 33; unpublished observations and discussed below). We therefore investigated the involvement of RIG-I in the TLR3-mediated signaling pathway. For this, we first used HeLa cells, which can be stimulated through TLR3 by the addition of poly(I:C) to the culture medium[30]. Alternatively, HeLa cells can be stimulated by cytoplasmic signaling triggered by viral infection. We transfected human IRF-3 tagged with p50 epitope into HeLa cells in the presence or absence of RIG-IC, which functions as a dominant negative inhibitor (**Fig. 3a**), stimulated cells with poly(I:C) or viral infection and analyzed cell lysates by native PAGE. Virus-induced activation of IRF-3 was inhibited by RIG-IC; however, induction by poly(I:C) treatment was unaffected (**Fig. 6a**). As an alternative model, we used 293T cells (**Fig. 6b**). The 293T cells did not show responsiveness to poly(I:C) added to the culture medium; however, ectopic expression of TLR3 conferred responsiveness to poly(I:C). NDV infection induced reporter gene expression in 293T cells irrespective of TLR3 expression. The dominant negative RIG-IC selectively blocked NDV-induced gene induction.

Trif is essential in the activation of IRF-3 triggered by TLR3 and TLR4 (refs. 29,32). Further downstream, TBK1 functions as an IRF-3 kinase[15–17]. We explored the involvement of these molecules by use of primary mouse embryonic fibroblasts (MEFs) derived from wild-type, TLR3-deficient, Trif-deficient and TBK1-deficient mice (**Fig. 7**). These mutant cells showed dimerization and nuclear translocation of IRF-3 after NDV infection similar to that of wild-type cells. The normal response of TBK1-deficient cells was unexpected, as we found reduced responsiveness in TBK1-deficient cells with a different culture history (H. Hemmi and S.A., unpublished observations). We confirmed the lack of TBK1 protein in the TBK1-deficient cells (**Supplementary Fig. 4** online). Although the existence of unidentified IRF-3 kinases was not strictly ruled out, we speculate that IKK-i, a structurally and functionally related kinase, compensated for the deficiency in the TBK1-deficient cells used in this experiment. In all these primary cells, ectopic expression of dominant negative RIG-IC blocked NDV-induced gene activation (**Fig. 7c**). These results suggest that TLR3- and RIG-I-mediated signals function independently.

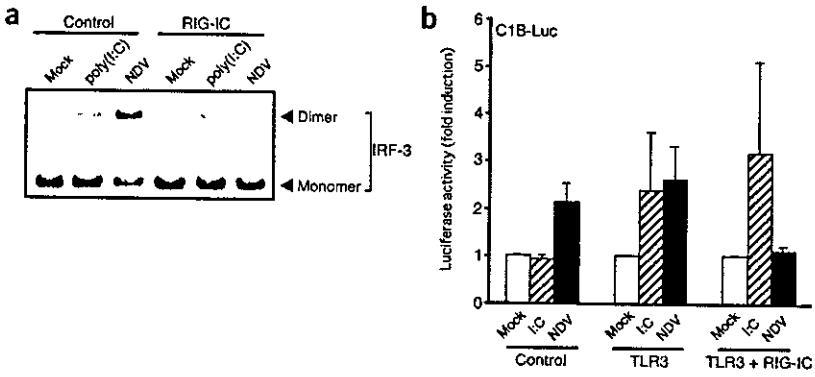

Figure 6 Dominant negative RIG-I inhibits NDV-induced but not TLR3-mediated activation of IRF-3. (a) HeLa cells were transiently transfected with p50-tagged IRF-3 along with either control vector (Control) or dominant negative RIG-I (RIG-IC). Cells were mock treated (Mock), stimulated by the addition of poly(I:C) to the culture medium for 1 h (poly(I:C)) or infected with NDV for 9 h (NDV). Lysates were separated by native PAGE and transfected IRF-3 was detected by immunoblot with anti-p50. (b) 293T cells were transiently transfected with p-55C1BLuc together with empty vector (Control), pEFTLR3 (TLR3) or pEFTLR3 and pEF-flagRIG-IC (TLR3 + RIG-IC). After 24 h of transfection, cells were split and were mock treated (Mock) or were induced by the addition of poly(I:C) in the medium (I:C; 20 μg/ml for 3 h) or by NDV infection (NDV; 12 h). Luciferase activity is presented as 'fold induction'. These results were reproducibly obtained in two independent transfection experiments. Error bars indicate triplicate samples of experiments.

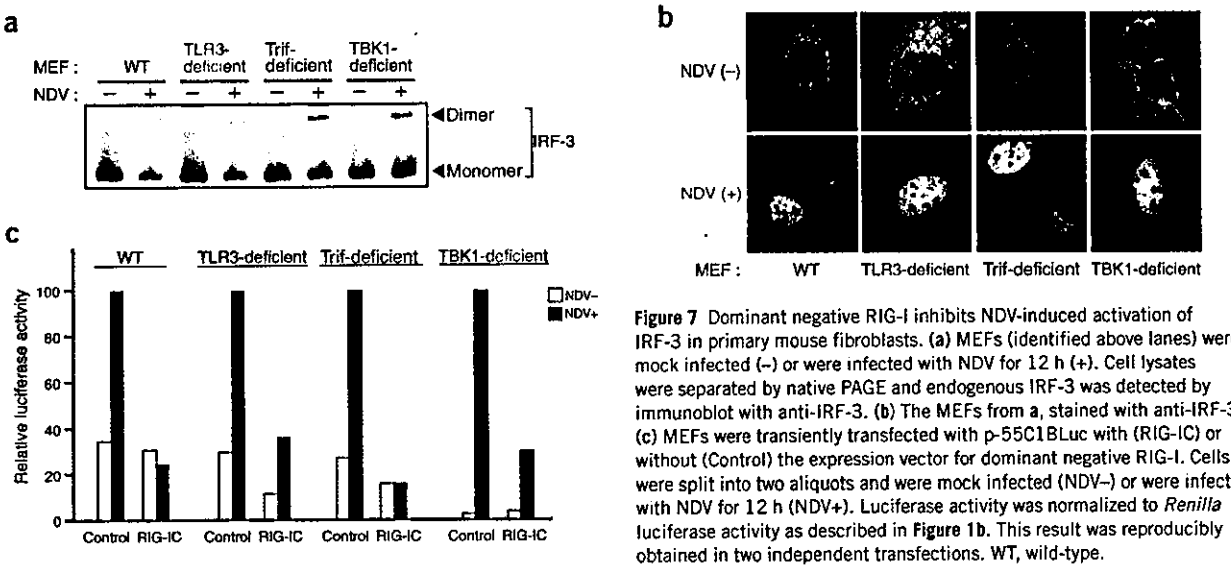

Figure 7 Dominant negative RIG-I inhibits NDV-induced activation of IRF-3 in primary mouse fibroblasts. (**a**) MEFs (identified above lanes) were mock infected (−) or were infected with NDV for 12 h (+). Cell lysates were separated by native PAGE and endogenous IRF-3 was detected by immunoblot with anti-IRF-3. (**b**) The MEFs from **a**, stained with anti-IRF-3. (**c**) MEFs were transiently transfected with p-55C1BLuc with (RIG-IC) or without (Control) the expression vector for dominant negative RIG-I. Cells were split into two aliquots and were mock infected (NDV−) or were infected with NDV for 12 h (NDV+). Luciferase activity was normalized to *Renilla* luciferase activity as described in **Figure 1b**. This result was reproducibly obtained in two independent transfections. WT, wild-type.

DISCUSSION

Here we used two independent cell lines and primary cells to obtain evidence that the DExD/H box helicase RIG-I mediated signals triggered by cytoplasmic dsRNA, resulting in activation of NF-κB and IRF-3, critical regulators of innate immune responses. This seems to be an alternative to TLR3-mediated signaling. Among the more than 100 helicases in the human genome, DExD/H box helicases may have the potential to unwind dsRNA by virtue of intrinsic ATPase activity[36]. Although their core sequence motifs are conserved, in overall structure these proteins diverge considerably. Thus, different helicases are linked to various biological processes such as transcription, translation, mRNA splicing and RNAi[36,37]. RIG-I is different from other helicases in containing two tandem CARD motifs. The CARD has been identified as a domain acting as an interface between molecules that signal the need for critical processes such as apoptosis and gene regulation[45]. We hypothesized that the CARD of RIG-I interacts with downstream molecules to further signaling. Consistent with this, overexpression of CARD alone activated the downstream signaling. Moreover, the mutant of RIG-I lacking CARD was not capable of transmitting signals. The CARDs of RIG-I, Nod1 and Nod2 activated NF-κB; however, activation of IRF-3 was selectively promoted by the CARD of RIG-I, suggesting target specificity of each CARD.

In the GenBank database we found another interferon-inducible, CARD-containing helicase, MDA5 (refs. 40,46), which is the closest relative of RIG-I, showing 23% and 35% amino acid identity in the N-terminal tandem CARD and C-terminal helicase domain, respectively. In our preliminary experiments, MDA5 CARD also augmented the constitutive as well as NDV- or dsRNA-stimulated expression of the C1B reporter gene, suggesting functional similarity for RIG-I and MDA5 in dsRNA-induced signaling. Furthermore, we found another DExD/H box RNA helicase, LGP2, in GenBank, which is homologous to the helicase portions of RIG-I (31% identity) and MDA5 (41% identity) but is completely devoid of a CARD. Like RIG-IC, LGP2 blocked signaling in certain conditions, suggesting it has a negative regulatory function (data not shown). Further examination is required to elucidate the overall picture of cytoplasmic dsRNA-mediated signaling pathway. A mouse locus has been identified that determines responsiveness to dsRNA in Trif-independent way[47]. Although this locus does not coincide with genes encoding any of the helicases described above, it is possible that the corresponding gene product expressed by this locus functions in signaling pathway triggered by RIG-I. In contrast, mouse TLR7 or human TLR8 recognizes viral single-stranded RNA or uridine-rich single-stranded RNA in the lysosomal compartment and activates expression of type I interferon in monocytes and macrophages[23–25]. As 293T cells apparently lack TLR7 (ref. 23) and MEFs did not respond to transfection of poly(U) (**Supplementary Fig. 5** online), the RIG-I-mediated signaling pathway is independent of TLR7.

Although the abundance of RIG-I protein was augmented considerably by interferon treatment, this effect was insufficient to activate signals downstream. This suggests that in physiological conditions, the CARD is under negative regulation as an integral part of the full-length protein. This hypothesis was supported by the observation that the mutant of RIG-I with a disrupted ATP-binding motif was unable to transmit signals downstream, irrespective of whether an intact CARD was retained. We speculate that this repression is caused by the C-terminal helicase domain. The repression is nonproteolytically reversed when the molecule is stimulated appropriately, such as by interaction with dsRNA. Indeed, RIG-I specifically recognizes dsRNA. However, physical interaction with dsRNA itself was not sufficient, as the mutation in the ATP-binding motif, which did not affect the dsRNA binding (data not shown), resulted in the generation of a dominant negative inhibitor. These results suggest that helicase activity is involved in the generation of signaling-competent RIG-I. A possible scenario for this is that dsRNA binds to the helicase domain, resulting in activation of the ATP-hydrolyzing function and a conformational change of the substrate dsRNA, helicase domain and CARD. Then the CARD is conferred an ability to transmit signals downstream by the recruitment of other molecules.

Ectopic expression of RIG-I alone could confer antiviral resistance to VSV and EMCV, which replicate differently in many ways but commonly produce dsRNA in cells. Stable RIG-I transformants do

not produce interferon constitutively; however, once viral dsRNA is generated in cells, primary activation of cytokines including interferon and subsequent secondary signaling by these cytokines may take place, thus resulting in the inhibition of viral replication. These results suggest a potential application for RIG-I for therapeutic and diagnostic purposes.

Organisms have mechanisms that detect and destroy infecting viruses. In plants, the main antiviral response is due to RNAi, in which several RNA helicases are reported to be involved[37]. In higher vertebrates, the interferon system is responsible for the early phase of innate immunity and is eventually taken over by antigen-specific acquired immune responses. Although the interferon system is restricted to vertebrates, primordial forms of its components, such as NF-κB and the transcription factor STAT, are found in invertebrates. The considerable structural conservation between the C-terminal domain of IRF-3 and the Mad homology domain 2 of the transcription factor Smad suggests an evolutional relationship between IRF-3 and Smad[48,49]. Dicer-related helicase 1 of *Caenorhabditis elegans*, which is homologous to RIG-I in the CARD and helicase domain, is essential in RNAi[50]. Thus, the interferon system and RNAi make use of RNA helicases to detect 'foreign' dsRNA to initiate their respective responses.

METHODS

Cells, DNA transfection, preparation of cell extracts and luciferase assay. K562 cells were cultured in RPMI 1641 medium supplemented with FBS (10%), penicillin (100 U/ml) and streptomycin (100 μg/ml). L929 cells were maintained in MEM with 5% FBS and penicillin-streptomycin. HeLa and 293T cells were maintained in DMEM with 10% FBS and penicillin-streptomycin. L929 and 293T cells were transiently transfected with the DEAE-dextran method and the calcium-phosphate method, respectively, as described[8]. MEFs were obtained from wild-type, TLR3-deficient, Trif-deficient[32] and TBK1-deficient (H. Hemmi and S.A., unpublished data) mice and were maintained in DMEM with FBS and penicillin-streptomycin. MEFs were transfected with FuGENE6 (Roche). Stable transformants of L929 cells were established by transfection of linearized empty vector (pEF-BOS) or expression plasmid for RIG-Ifull (pEF-flagRIG-Ifull) with pCDM8neo, followed by selection with G418 (1 mg/ml). NDV infection and poly(I:C) transfection were done as reported[8]. For preparation of cell extracts, cells were lysed with lysis buffer (50 mM Tris-HCl pH 7.5, 150 mM NaCl, 1 mM EDTA, 1% Nonidet P-40, 0.1 mg/ml of leupeptin, 1 mM phenylmethylsulfonyl fluoride and 1 mM sodium orthovanadate) and were centrifuged at 245,000*g* for 10 min. The supernatant was used for immunoblots, electrophoretic mobility-shift assay (EMSA) and poly(I:C) 'pulldown' assay. The Dual-Luciferase Reporter Assay System (Promega) was used for luciferase assays. As internal control for the Dual-Luciferase assay, the *Renilla* luciferase construct pRL-TK (Promega) was used.

Molecular cloning of ΔRIG-I. We generated an expression cDNA library with the Creator SMART cDNA Library Construction kit (Clontech) with several modifications. The mRNA of IFN-β-treated (1×10^3 IU/ml for 10 h) K562 cells was prepared with TRIzol (Gibco) and an mRNA Purification kit (Amersham). The synthesized cDNA was introduced into pEF-BOS at two *Sfi*I sites generated by the insertion of oligonucleotides. The library was split into about 5,000 pools containing 20 independent clones each (total, 1×10^5 clones), and plasmid DNA was prepared with NucleoSpin Robot-96 Plasmid (Macherey-Nagel). L929 cells were seeded into 96-well plates (5×10^4 cells/well) and were transfected with p-55C1BLuc (100 ng), pRL-TK (1 ng) and library DNA (~300 ng). At 24 h after transfection, cells were stimulated by poly(I:C) transfection for 6 h and were subjected to the Dual-Luciferase assay. The cDNA clones with enhanced luciferase activity were isolated from the pools by the same assay.

Plasmid constructs. The p-55C1BLuc, p-125Luc, p-55A2Luc, p-55UAS$_G$Luc, pEFGal4–IRF-3 and pEF-flagTLR3 plasmids have been described[8,31]. The cDNA for RIG-I, Nod1, Nod2 and eIF-4A was isolated by RT-PCR and inserted into the *Xba*I-*Cla*I sites of pEF-BOS(+), constructed by the insertion of multiple cloning sequences at the *Xba*I site, with oligonucleotides for N-terminal FLAG tag (pEF-flagRIG-I, pEF-flagNod1N, pEF-flagNod2CARD and pEF-flageIF-4A). The nucleotide sequence for the entire cDNA of each was confirmed with the BigDye DNA sequencing kit (Applied Biosystems). Deleted and site-directed mutants were obtained by insertion of the appropriate oligonucleotides and the Kunkel method[51], respectively (pEF-flagRIG-IC and pEF-flagRIG-IKA).

EMSA. These assays were done as described[8].

Antibodies, enzyme-linked immunosorbent assay (ELISA), immunoblots and immunostaining. Anti-RIG-I, anti-mouse IRF-3, anti-p50-tag and anti-mouse type I interferon antibodies have been described[8,52,53]. The monoclonal antibodies to FLAG (M2, SIGMA) and actin (Chemicon) are commercial products. Culture supernatants of transfected 293T cells were subjected to ELISA with a human IFN-β ELISA kit (Fujirebio). SDS-PAGE, native PAGE and immunoblots were done as described[8,54]. To detect RIG-I, we used horseradish peroxidase–conjugated protein A (Amersham) and an ECL Plus detection system (Amersham). Immunostaining was done as described[8] with anti-mouse IRF-3.

The poly(I:C) 'pulldown' assay. Cell lysates extracted from transfected 293T cells were mixed for 1 h at 4 °C with poly(I:C)-agarose (Amersham), washed extensively with lysis buffer and separated by SDS-PAGE, followed by immunoblot with anti-FLAG. For competition assays, poly(I:C), poly(rA):poly(rU), poly(A) or sonicated herring sperm DNA (dsDNA) was added to the binding reaction at a specified concentration.

RNAi. RNAi vectors were constructed by the insertion of oligonucleotides into *Bsp*MI sites of the piGENE hU6 as described[55]. The target sequences for siRNA are 5′-GAATTTAAAACCAGAATTATC-3′ (control, human RIG-I sequence, which diverges considerably from the mouse) and 5′-GCCCATTGAAACCAAGAAATT-3′ (mouse RIG-I). Mouse L929 cells (1×10^6) were transfected with RNAi vector (10 μg) together with a puromycin-resistance gene (1 μg) with the *Trans*IT-LT1 transfection reagent (Mirus). After incubation for 87 h in the presence of puromycin (10 μg/ml), cells were infected for 9 h with NDV. Cell extracts were separated by SDS-PAGE or native PAGE and endogenous RIG-I, actin and IRF-3 were detected by immunoblot. Total RNA was prepared with TRIzol reagent (Gibco), treated with DNase I (Roche) and amplified by real-time PCR with the ABI PRISM 7700 Sequence Detection System (Applied Biosystems). TaqMan Reverse Transcription reagents and the TaqMan Universal PCR Mix (Applied Biosystems) were used for cDNA synthesis and PCR, respectively. We used commercial TaqMan primer-probe sets (Applied Biosystems) for mouse *Ifnb*, *Cxcl10* and *Ccl5*. To detect IFN-α4 mRNA, we used the primer-probe set reported[56]. As an internal control for the comparative threshold cycle method, a primer-probe set for eukaryotic 18S rRNA (Applied Biosystems) was used.

Virus infection and plaque assay. L929-derived stable transformants were treated with culture medium ('mock-infected') throughout for all experiments or were infected with VSV or EMCV. Culture supernatants were recovered and cells were stained with amido black. Virus yield in culture supernatants was determined by standard plaque assay. Freshly prepared L929 cells were infected with serial dilutions of the recovered viruses. The cells were overlaid with MEM containing 1% agarose and were incubated for 24 h. Vital staining was done with neutral red and plaques were counted.

Note: Supplementary information is available on the Nature Immunology website.

ACKNOWLEDGMENTS

We thank E.L. Barsoumian for critical reading of the manuscript; S. Saito and M. Kohase for plaque assay protocol and suggestions; and M. Kohara for suggestions on real-time PCR. Supported by the Research for the Future Program; Japan Society for the Promotion of Science; Ministry of Education, Culture, Sports, Science and Technology of Japan; Nippon Boehringer Ingelheim; and Toray Industries.

COMPETING INTERESTS STATEMENT

The authors declare competing financial interests (see the *Nature Immunology* website for details).

Received 20 January; accepted 5 May 2004
Published online at http://www.nature.com/natureimmunology/

1. De Maeyer, E. & De Maeyer-Guignard, J. Type I interferons. *Int. Rev. Immunol.* **17**, 53–73 (1998).
2. Farrar, J.D. & Murphy, K.M. Type I interferons and T helper development. *Immunol. Today* **21**, 484–489 (2000).
3. Samuel, C.E. Antiviral actions of interferons. *Clin. Microbiol. Rev.* **14**, 778–809 (2001).
4. Lin, R., Heylbroeck, C., Pitha, P.M. & Hiscott, J. Virus-dependent phosphorylation of the IRF-3 transcription factor regulates nuclear translocation, transactivation potential, and proteasome-mediated degradation. *Mol. Cell. Biol.* **18**, 2986–2996 (1998).
5. Sato, M., Tanaka, N., Hata, N., Oda, E. & Taniguchi, T. Involvement of the IRF family transcription factor IRF-3 in virus-induced activation of the IFN-β gene. *FEBS Lett.* **425**, 112–116 (1998).
6. Wathelet, M.G. *et al.* Virus infection induces the assembly of coordinately activated transcription factors on the IFN-β enhancer *in vivo*. *Mol. Cell* **1**, 507–518 (1998).
7. Weaver, B.K., Kumar, K.P. & Reich, N.C. Interferon regulatory factor 3 and CREB-binding protein/p300 are subunits of double-stranded RNA-activated transcription factor DRAF1. *Mol. Cell. Biol.* **18**, 1359–1368 (1998).
8. Yoneyama, M. *et al.* Direct triggering of the type I interferon system by virus infection: activation of a transcription factor complex containing IRF-3 and CBP/p300. *EMBO J.* **17**, 1087–1095 (1998).
9. Fujita, T., Miyamoto, M., Kimura, Y., Hammer, J. & Taniguchi, T. Involvement of a *cis*-element that binds an H2TF-1/NF-κB like factor(s) in the virus-induced interferon-β gene expression. *Nucl. Acids Res.* **17**, 3335–3346 (1989).
10. Lenardo, M.J., Fan, C.M., Maniatis, T. & Baltimore, D. The involvement of NF-κB in β-interferon gene regulation reveals its role as widely inducible mediator of signal transduction. *Cell* **57**, 287–294 (1989).
11. Visvanathan, K.V. & Goodbourn, S. Double-stranded RNA activates binding of NF-κB to an inducible element in the human β-interferon promoter. *EMBO J.* **8**, 1129–1138 (1989).
12. Du, W. & Maniatis, T. An ATF/CREB binding site is required for virus induction of the human interferon β gene. *Proc. Natl. Acad. Sci. USA* **89**, 2150–2154 (1992).
13. Sato, M. *et al.* Distinct and essential roles of transcription factors IRF-3 and IRF-7 in response to viruses for IFN-α/β gene induction. *Immunity* **13**, 539–548 (2000).
14. Suhara, W., Yoneyama, M., Kitabayashi, I. & Fujita, T. Direct involvement of CREB-binding protein/p300 in sequence-specific DNA binding of virus-activated interferon regulatory factor-3 holocomplex. *J. Biol. Chem.* **277**, 22304–22313 (2002).
15. Fitzgerald, K.A. *et al.* IKKε and TBK1 are essential components of the IRF3 signaling pathway. *Nat. Immunol.* **4**, 491–496 (2003).
16. Sharma, S. *et al.* Triggering the interferon antiviral response through an IKK-related pathway. *Science* **300**, 1148–1151 (2003).
17. McWhirter, S.M. *et al.* IFN-regulatory factor 3-dependent gene expression is defective in Tbk1-deficient mouse embryonic fibroblasts. *Proc. Natl. Acad. Sci. USA* **101**, 233–238 (2004).
18. Krieg, A.M. CpG motifs in bacterial DNA and their immune effects. *Annu. Rev. Immunol.* **20**, 709–760 (2002).
19. Sing, A. *et al.* Bacterial induction of β interferon in mice is a function of the lipopolysaccharide component. *Infect. Immun.* **68**, 1600–1607 (2000).
20. Alexopoulou, L., Holt, A.C., Medzhitov, R. & Flavell, R.A. Recognition of double-stranded RNA and activation of NF-κB by Toll-like receptor 3. *Nature* **413**, 732–738 (2001).
21. Poltorak, A. *et al.* Defective LPS signaling in C3H/HeJ and C57BL/10ScCr mice: mutations in Tlr4 gene. *Science* **282**, 2085–2088 (1998).
22. Hoshino, K. *et al.* Cutting edge: Toll-like receptor 4 (TLR4)-deficient mice are hyporesponsive to lipopolysaccharide: evidence for TLR4 as the *Lps* gene product. *J. Immunol.* **162**, 3749–3752 (1999).
23. Heil, F. *et al.* Species-specific recognition of single-stranded RNA via Toll-like receptor 7 and 8. *Science* **303**, 1526–1529 (2004).
24. Diebold, S.S., Kaisho, T., Hemmi, H., Akira, S. & Reis, E.S.C. Innate antiviral responses by means of TLR7-mediated recognition of single-stranded RNA. *Science* **303**, 1529–1531 (2004).
25. Lund, J.M. *et al.* Recognition of single-stranded RNA viruses by Toll-like receptor 7. *Proc. Natl. Acad. Sci. USA* **101**, 5598–5603 (2004).
26. Hemmi, H. *et al.* A Toll-like receptor recognizes bacterial DNA. *Nature* **408**, 740–745 (2000).
27. Akira, S., Takeda, K. & Kaisho, T. Toll-like receptors: critical proteins linking innate and acquired immunity. *Nat. Immunol.* **2**, 675–680 (2001).
28. Hoshino, K., Kaisho, T., Iwabe, T., Takeuchi, O. & Akira, S. Differential involvement of IFN-β in Toll-like receptor-stimulated dendritic cell activation. *Int. Immunol.* **14**, 1225–1231 (2002).
29. Hoebe, K. *et al.* Identification of Lps2 as a key transducer of MyD88-independent TIR signalling. *Nature* **424**, 743–748 (2003).
30. Oshiumi, H., Matsumoto, M., Funami, K., Akazawa, T. & Seya, T. TICAM-1, an adaptor molecule that participates in Toll-like receptor 3-mediated interferon-β induction. *Nat. Immunol.* **4**, 161–167 (2003).
31. Yamamoto, M. *et al.* Cutting edge: a novel Toll/IL-1 receptor domain-containing adapter that preferentially activates the IFN-β promoter in the Toll-like receptor signaling. *J. Immunol.* **169**, 6668–6672 (2002).
32. Yamamoto, M. *et al.* Role of adaptor TRIF in the MyD88-independent toll-like receptor signaling pathway. *Science* **301**, 640–643 (2003).
33. Diebold, S.S. *et al.* Viral infection switches non-plasmacytoid dendritic cells into high interferon producers. *Nature* **424**, 324–328 (2003).
34. Smith, E.J., Marie, I., Prakash, A., Garcia-Sastre, A. & Levy, D.E. IRF3 and IRF7 phosphorylation in virus-infected cells does not require double-stranded RNA-dependent protein kinase R or IκB kinase but is blocked by vaccinia virus E3L protein. *J. Biol. Chem.* **278**, 8951–8957 (2001).
35. Iwamura, T. *et al.* PACT, a double-stranded RNA binding protein acts as a positive regulator for type I interferon gene induced by Newcastle disease virus. *Biochem. Biophys. Res. Commun.* **282**, 515–523 (2001).
36. Tanner, N.K. & Linder, P. DExD/H box RNA helicases: from generic motors to specific dissociation functions. *Mol. Cell* **8**, 251–262 (2001).
37. Tijsterman, M., Ketting, R.F. & Plasterk, R.H. The genetics of RNA silencing. *Annu. Rev. Genet.* **36**, 489–519 (2002).
38. Sun, Y.W. RIG-I, a Human Homolog Gene of RNA Helicase, Is Induced by Retinoic Acid During the Differentiation of Acute Promyelocytic Leukemia Cell. Thesis, Shanghai Second Medical Univ. (1997).
39. Zhang, X., Wang, C., Schook, L.B., Hawken, R.J. & Rutherford, M.S. An RNA helicase, RHIV-1, induced by porcine reproductive and respiratory syndrome virus (PRRSV) is mapped on porcine chromosome 10q13. *Microb. Pathog.* **28**, 267–278 (2000).
40. Kang, D.C. *et al.* mda-5: An interferon-inducible putative RNA helicase with double-stranded RNA-dependent ATPase activity and melanoma growth-suppressive properties. *Proc. Natl. Acad. Sci. USA* **99**, 637–642 (2002).
41. Inohara, N. & Nunez, G. NODs: intracellular proteins involved in inflammation and apoptosis. *Nat. Rev. Immunol.* **3**, 371–382 (2003).
42. Ogura, Y. *et al.* Nod2, a Nod1/Apaf-1 family member that is restricted to monocytes and activates NF-κB. *J. Biol. Chem.* **276**, 4812–4818 (2001).
43. Watanabe, N., Sakakibara, J., Hovanessian, A.G., Taniguchi, T. & Fujita, T. Activation of IFN-β element by IRF-1 requires a posttranslational event in addition to IRF-1 synthesis. *Nucl. Acids Res.* **19**, 4421–4428 (1991).
44. Walker, J.E., Saraste, M., Runswick, M.J. & Gay, N.J. Distantly related sequences in the α- and β-subunits of ATP synthase, myosin, kinases and other ATP-requiring enzymes and a common nucleotide binding fold. *EMBO J.* **1**, 945–951 (1982).
45. Bouchier-Hayes, L. & Martin, S.J. CARD games in apoptosis and immunity. *EMBO Rep.* **3**, 616–621 (2002).
46. Kovacsovics, M. *et al.* Overexpression of Helicard, a CARD-containing helicase cleaved during apoptosis, accelerates DNA degradation. *Curr. Biol.* **12**, 838–843 (2002).
47. Hoebe, K. *et al.* Upregulation of costimulatory molecules induced by lipopolysaccharide and double-stranded RNA occurs by Trif-dependent and Trif-independent pathways. *Nat. Immunol.* **4**, 1223–1229 (2003).
48. Takahasi, K. *et al.* X-ray crystal structure of IRF-3 and its functional implications. *Nat. Struct. Biol.* **10**, 922–927 (2003).
49. Qin, B.Y. *et al.* Crystal structure of IRF-3 reveals mechanism of autoinhibition and virus-induced phosphoactivation. *Nat. Struct. Biol.* **10**, 913–921 (2003).
50. Tabara, H., Yigit, E., Siomi, H. & Mello, C.C. The dsRNA binding protein RDE-4 interacts with RDE-1, DCR-1, and a DExH-box helicase to direct RNAi in *C. elegans*. *Cell* **109**, 861–871 (2002).
51. Kunkel, T.A. Rapid and efficient site-specific mutagenesis without phenotypic selection. *Proc. Natl. Acad. Sci. USA* **82**, 488–492 (1985).
52. Imaizumi, T. *et al.* Retinoic acid-inducible gene-I is induced in endothelial cells by LPS and regulates expression of COX-2. *Biochem. Biophys. Res. Commun.* **292**, 274–279 (2002).
53. Yoneyama, M. *et al.* Autocrine amplification of type I interferon gene expression mediated by interferon stimulated gene factor 3 (ISGF3). *J. Biochem. (Tokyo)* **120**, 160–169 (1996).
54. Mori, M. *et al.* Identification of Ser-386 of interferon regulatory factor 3 as critical target for inducible phosphorylation that determines activation. *J. Biol. Chem.* **279**, 9698–9702 (2004).
55. Miyagishi, M. & Taira, K. Strategies for generation of an siRNA expression library directed against the human genome. *Oligonucleotides* **13**, 325–333 (2003).
56. Karaghiosoff, M. *et al.* Central role for type I interferons and Tyk2 in lipopolysaccharide-induced endotoxin shock. *Nat. Immunol.* **4**, 471–477 (2003).

Published online 23 April 2004

Nucleic Acids Research, 2004, Vol. 32, No. 7 e66
DOI: 10.1093/nar/gnh061

Control of siRNA expression using the Cre–*loxP* recombination system

Vivi Kasim[1], Makoto Miyagishi[1,2] and Kazunari Taira[1,2,*]

[1]Department of Chemistry and Biotechnology, School of Engineering, University of Tokyo, Hongo, Tokyo 113-8656, Japan and [2]Gene Function Research Center, National Institute of Advanced Industrial Science and Technology (AIST), Central 4, 1-1-1 Higashi, Tsukuba Science City 305-8562, Japan

Received February 24, 2004; Revised and Accepted March 24, 2004

ABSTRACT

Gene silencing mediated by RNA interference (RNAi) was first discovered in *Caenorhabditis elegans*, and was subsequently recognized in various other organisms. In mammalian cells, RNAi can be induced by small interfering RNAs (siRNAs). In earlier studies, our group developed a vector-based system for expression of siRNA under control of a polymerase III promoter, the U6 promoter, which can induce RNAi in living cells. We here describe a system for controlling the U6 promoter-driven expression of siRNA using the Cre–*loxP* recombination system. We constructed a 'Cre-On' siRNA expression vector which could be switched on upon excision catalyzed by Cre recombinase, which was delivered to cells directly from the medium as a fusion protein. An examination of the effectiveness of RNAi against a reporter gene revealed that addition of TAT-NLS-Cre (where NLS is a nuclear localization signal and TAT is a peptide of 11 amino acids derived from HIV) to the medium resulted in plasmid recombination, generation of siRNA and suppression of reporter activity. This system should allow us to induce RNAi in a spatially, temporally, cell type-specifically or tissue-specifically controlled manner and potentiate the improved application of RNAi in both an experimental and a therapeutic context.

INTRODUCTION

RNA interference (RNAi) is a post-transcriptional gene silencing phenomenon induced by double-stranded RNA (dsRNA) that was first discovered in *Caenorhabditis elegans* (1). In RNAi, it appears that dsRNAs are cleaved by a member of the RNase III family (Dicer) into small interfering RNAs (siRNAs) of 21 or 22 nt in length (2–4), which in turn induce the degradation of the target mRNA, with resultant suppression of expression of the target gene. This phenomenon has been found in evolutionarily diverse organisms, such as plants, a nematode, the fruit fly and a protozoan (5–8). In the case of mammalian cells, it was reported initially that dsRNAs cause the non-specific degradation of mRNA, but now it is clear that 21 or 22 nt RNAs with 2 or 3 nt 3′ overhangs, known as small interfering RNAs (siRNAs), induce RNAi in cultured mammalian cells without inducing the dsRNA-dependent non-specific inhibition of protein synthesis (2,9,10). Various groups, including our own, have developed vector-mediated systems for specific RNAi in mammalian cells using polymerase (pol) III promoters such as the U6, H1 and $tRNA^{Val}$ promoters (11–18). Furthermore, both synthetic siRNAs and small hairpin RNAs transcribed *in vivo* can successfully suppress the expression of transgenes and an endogenous gene in adult mice (19–21).

Today, RNAi shows considerable promise as both an experimental and a therapeutic tool. Suppression of the expression of a gene of interest by RNAi has several positive features. Such a system is easy to design, exhibits strong site specificity and has a strong suppressive effect. Moreover, only low concentrations of siRNA are required. To make RNAi a more efficient tool, for example for the study of genes that are essential for survival, and for cell type-specific, tissue-specific and time–course experiments, it is necessary to control the expression of siRNA both spatially and temporally. siRNA expression systems using a pol II or a pol III promoter that can be regulated by tetracycline have been reported (22–26) but, to our knowledge, there have been no reports of the control of expression of pol III promoter-based siRNA expression vectors using a Cre–*loxP* system with exogenously introduced Cre recombinase fusion proteins.

The Cre–*loxP* system is a system that is widely used in reverse genetics. The Cre recombinase is a site-specific recombinase encoded by bacteriophage P1 that recognizes and promotes recombination at *loxP* sites (27), which consist of two 13 bp repeats, each separated by an 8 bp spacer region. Direct repeats of *loxP* result in excision, while inverted repeats cause inversion of the sequence placed between them (28). Cre-mediated recombination can be achieved in various kinds of eukaryotic cell, such as yeast (29), plant (30) and mammalian cells (31). Furthermore, Cre recombinase can also be stably expressed in transgenic mice (32,33).

*To whom correspondence should be addressed at Department of Chemistry and Biotechnology, School of Engineering, University of Tokyo, Hongo, Tokyo 113-8656, Japan. Tel: +81 3 5841 8828; Fax: +81 3 5841 7340; Email: taira@chembio.t.u-tokyo.ac.jp

The authors wish it to be known that, in their opinion, the first two authors should be regarded as joint First Authors